



Methodology for Regional Multihazard Hurricane Damage and Risk Assessment

Omar M. Nofal, S.M.ASCE¹; John W. van de Lindt, F.ASCE²; Trung Q. Do, M.ASCE³; Guirong Yan, M.ASCE⁴; Sara Hamideh, M.ASCE⁵; Daniel T. Cox, M.ASCE⁶; and J. Casey Dietrich, M.ASCE⁷

Abstract: Hurricanes are devastating natural hazards that often cause damage to the built environment as a result of their loadings, which include storm surge, waves, and wind, often in combination. Modeling these hazards individually and their effects on buildings is a complex process because each loading component within the hazard behaves differently, affecting either the building envelope, the structural system, or the interior contents. Realistic modeling of hurricane effects requires a multihazard approach that considers the combined effects of wind, surge, and waves. Previous studies focused primarily on modeling these hazards individually, with less focus on the multihazard impact on the whole building system made up of the combination of the structure and its interior contents. The analysis resolution used in previous studies did not fully enable hurricane risk assessment through a detailed investigation of the vulnerability at the component-level or subassembly-level (a group of components such as interior contents, structural components, or nonstructural components). To address these research gaps, a robust multihazard hurricane risk analysis model that uses high-resolution hazard, exposure, and vulnerability models was developed. This model uses a novel approach to combine the storm surge and wave fragility functions with a suite of existing wind fragilities to account for structural damage and then combines them with another suite of flood-based fragilities to account for interior content damage. The proposed vulnerability model was applied to the state of North Carolina as an example of a regional-scale assessment to demonstrate the ability of the method to predict damage at the building level across this large spatial domain. This model enables better understanding of the damages caused by hurricanes in coastal regions, thereby setting initial postimpact conditions for community resilience assessment and investigation of recovery policy alternatives. DOI: 10.1061/(ASCE)ST.1943-541X.0003144. © 2021 American Society of Civil Engineers.

Author keywords: Hurricane vulnerability; Fragility analysis; Multihazard hurricane; Damage analysis; Loss analysis.

Introduction

Hurricanes are multihazard events that bring strong winds, storm surge, and waves, exposing the physical infrastructure within

¹Ph.D. Candidate, Dept. of Civil and Environmental Engineering, Colorado State Univ., Fort Collins, CO 80523. ORCID: https://orcid.org/0000-0003-4206-1904. Email: omar.nofal@colostate.edu

²Harold H. Short Endowed Chair Professor and Co-Director, Center of Excellence for Risk-Based Community Resilience Planning, Dept. of Civil and Environmental Engineering, Colorado State Univ., Fort Collins, CO 80523 (corresponding author). Email: jwv@engr.colostate.edu

³Visiting Assistant Professor, Dept. of Civil Engineering, Univ. of Louisiana at Lafayette, Lafayette, LA 70503. Email: trung.do@louisianana.edu

⁴Associate Professor, Dept. of Civil, Architectural and Environmental Engineering, Missouri Univ. of Science and Technology, St. Rolla, MO 65409. Email: yang@mst.edu

⁵Assistant Professor, School of Marine and Atmospheric Sciences, Stony Brook Univ., New York, NY 11790. Email: sara.hamideh@stonybrook.edu

⁶CH2M Hill Professor in Civil Engineering, Dept. of Civil and Construction Engineering, Oregon State Univ., Corvallis, OR 97331. Email: dan.cox@oregonstate.edu

Associate Professor, Dept. of Civil, Construction, and Environmental Engineering, North Carolina State Univ., Raleigh, NC 27607. ORCID: https://orcid.org/0000-0001-5294-2874. Email: jcdietrich@ncsu.edu

Note. This manuscript was submitted on January 12, 2021; approved on June 2, 2021; published online on August 30, 2021. Discussion period open until January 30, 2022; separate discussions must be submitted for individual papers. This paper is part of the *Journal of Structural Engineering*, © ASCE, ISSN 0733-9445.

coastal communities to different types of loadings and result in significant damage to the built environment (Nofal 2021). Hurricaneinduced winds can cause damage to the building system. Storm surge driven by hurricanes results in significant content and structural damage and can collapse buildings due to hydrostatic and hydrodynamic loadings, particularly when waves are present (Tomiczek et al. 2014). The impact of the combined hazards driven by hurricanes on buildings is very complex, depending on hazard characteristics which can vary across the coastline. Several recent studies focused on the combination of wind, wave, and surge/ coastal flooding (Ding et al. 2016; Masoomi et al. 2019), but it still is unclear how to separate damage from wind, wave, and/or surge when they occur simultaneously during a hurricane event. Buildings on the coastline are vulnerable to wind, waves, and storm surge, which cause different types of damage, including structural and contents damage from the combined surge, waves, and wind loads. Moving inland, hydrodynamic impacts decrease quickly, and the storm surge behaves more like coastal flooding, with the buildings subjected to effects from the combination of wind and flood. When storm surge no longer is present farther inland, buildings are affected primarily by wind and rain-driven flooding. However, this paper focuses on hurricane wind, waves, and surge for near-coast structures.

The literature related to hurricane-induced hazards and their associated risk on the built environment investigated the impacts of these hazards as single or combined loads on buildings. A number of researchers have investigated wind loads driven by hurricanes in terms of hazard modeling (Guo and van de Lindt 2019; Vickery et al. 2006a, 2009), building performance (Aghababaei et al. 2018; He et al. 2017; Pita et al. 2012), and loss estimation

(Kakareko et al. 2021; Khajwal and Noshadravan 2020; Li and Ellingwood 2006; Mishra et al. 2017; Vickery et al. 2006b). Combined wind and windborne debris damage models were developed over the last decade (Chung Yau et al. 2011; Grayson et al. 2013). A component-based surge vulnerability analysis has been pursued to develop fragility functions based on buildings and storm surge parameters (Hatzikyriakou et al. 2016). The joint impact of wind and storm surge induced by hurricanes has been investigated using stochastic hurricane models (Bushra et al. 2019; Pei et al. 2013, 2014; Unnikrishnan and Barbato 2017). A combined wind, rainwater intrusion, and storm surge loss analysis was investigated by several researchers using assembly-based vulnerability methods (Li et al. 2012; Park et al. 2013, 2014) and other probabilistic methods (Baradaranshoraka et al. 2017). The impact of combined waves and storm surge also was investigated with a focus on hazard modeling (Dietrich et al. 2011) and loss estimation (Do et al. 2020; Tomiczek et al. 2014, 2017). The impact of the different types of flooding on buildings and infrastructure including inland and coastal flooding induced by hurricanes also was investigated (Nofal and van de Lindt 2020c, d). Several hurricane multihazard models were developed to account for the combined impacts of wind, wave, and storm surge on buildings to develop fragility functions for wood-frame structures (Masoomi et al. 2019; Massarra et al. 2019; Nofal et al. 2021; van Verseveld et al. 2015) and performance-based hurricane engineering models (Barbato et al. 2013; McCullough et al. 2013). The Florida Public Hurricane Loss Model (FPHLM) provides a multidisciplinary system to account for the insured losses resulting from hurricane-induced hazards (Chen et al. 2009; FPHLM 2015).

The different models used to estimate the vulnerability of the built environment to hurricane-induced loads were reviewed by Pita et al. (2015). The review showed that probabilistic vulnerability models for hurricane-induced hazards were the focus of the literature over the last 2 decades (Abdelhady et al. 2020; Do et al. 2020; Henderson and Ginger 2007; Kakareko et al. 2021; Khajwal and Noshadravan 2020; Li and Ellingwood 2006; Mishra et al. 2017; Paleo-Torres et al. 2020; Pinelli et al. 2004; Wang et al. 2017; Zhang et al. 2018). Fragility functions were shown to be the most reliable probabilistic vulnerability functions that could inform probabilistic safety margins for buildings and systems (Ellingwood et al. 2004; Nofal and van de Lindt 2020a, d, 2021a, b; Rosowsky and Ellingwood 2002). Li and Ellingwood (2006) developed a probabilistic framework using fragility functions to evaluate residential buildings subjected to hurricane-induced wind. Probabilistic hurricane wind vulnerability models were developed using Bayesian capacity models to propagate uncertainties in the damage analysis (Kakareko et al. 2021; Mishra et al. 2017). Multihazard fragility-based hurricane damage models also were developed for combined hurricane storm surge and wave (Do et al. 2020; Masoomi et al. 2019). For community-level analysis, Abdelhady et al. (2018) investigated community resilience in the context of hurricane-induced hazards using a distributed computing platform. Additionally, the concept of vulnerability function portfolios was introduced in the literature to assess community-level performance (Lin and Wang 2016; Zhang et al. 2018). This allowed for multiple portfolios to be developed across multiple hazards, including wind (Memari et al. 2018) and flooding (Nofal and van de Lindt 2020b), and initiated several community resilience analysis studies (Nofal and van de Lindt 2020a, 2021b; Wang and van de Lindt 2021; Wang et al. 2021).

Although those studies provided detailed insight into the multiple hazards driven by hurricanes and their impacts on buildings and infrastructure, the literature still lacks a comprehensive approach that accounts for the combined impact of these multiple hazards at large spatial scales but with high resolution, such as at city or state level. The spatiotemporal variation of hurricane-induced hazards in terms of hazard intensity and type for coastal and inland communities and the coarse analysis resolution in many models makes it challenging to develop a multihazard hurricane vulnerability model to use at a large spatial scale. Each building on the coast may be subjected to one or multiple loadings at the same time or in succession with different intensities, resulting in cascading damages. A building-level approach would enable the information needed for communities to make risk-informed decisions of the hazard impacts across the community. Furthermore, most current vulnerability models account only for structural damage, and do not account for the contents damage resulting from the contact of surge with the building's interior contents. Although a building's interior contents may exceed half of the building market value, their damage assessment has not received adequate research attention compared with the structural system. Current flood damage models are based on a qualitative and empirical assessment that does not allow uncertainty propagation across the damage model. For example, the Hazus-MH hurricane model uses an assembly-based approach to account for contents damage resulting from flooding based on empirical assessment (FEMA 2003). Then the loss subassemblies from wind and flood hazards are combined in a single loss matrix. Although this approach is used widely in the US, it depends on empirical deterministic stage-damage functions with inherent uncertainties in the damage models. Therefore, a community-level multihazard probabilistic hurricane risk assessment model is needed to account for the collective impacts of the multihazards driven by hurricanes on both the building system and the interior contents.

This study presents a high-resolution multihazard hurricane risk analysis methodology which accounts for damage and loss at the individual building level. The methodology summarized herein uses a portfolio of building archetypes that represent typical communities in the US to extend its application for large-scale damage and loss assessment at the regional level. This method accounts for the combined impact of the main hazards driven by hurricanes (wind, wave, and storm surge) on buildings. The novel contributions of this paper are (1) the proposed probabilistic hurricane risk model accounts for both contents and structural damage resulting from the multiple hazards induced by hurricanes; and (2) a new approach of combining fragilities based on an array of intensity parameters is presented. This methodology requires a full realization of the vulnerability of the exposed buildings corresponding to each hazard type, along with a comprehensive understanding of the hurricane hazard mechanism and how it makes landfall (such as hurricane path, wind field, wind speed, surge height, wave height, and so forth) as well as building characteristics [e.g., location, number of stories, first-floor elevation, roof shape, foundation type, and construction material (including the type of building envelope), and so forth], and building vulnerability functions (fragility or loss functions). This building-level methodology will allow for better damage quantification by including the damage contribution from each hazard induced by hurricanes, thereby enabling decision support at the community and regional levels.

Methodology

A novel regional-scale multihazard hurricane risk analysis model was developed herein to account for the damage resulting from the multiple hazards driven by hurricanes. This study focused on the direct impact of the combined surge, wave, and wind on the building structural and contents damage. The impact of other

hazards driven by hurricanes such as the wind-rainfall intrusion contents damage and damage from windborne debris is beyond the scope of this study and is not included. Fig. 1 is a schematic representation of the hurricane risk analysis process and lays out the main components of the multiple hazards driven by hurricanes and their associated exposure and vulnerability. The hurricane exposure is divided into three zones based on the hazard that is dominant in that zone, namely the surge-wave-wind zone, the surge-wind zone, and the wind zone. The hurricane vulnerability analysis for each of these zones is calculated using fragility functions to describe building damage in terms of the exceedance probability of predefined damage states (DS). An innovative convolutional vulnerability model is proposed using well-established fragility functions from the literature for wind, wave, and surge. This vulnerability model captures the convolutional impacts of the spatiotemporal variation of hurricane-induced loading including surge, wave, and wind on the different building components including structural and nonstructural components and interior contents. The concept of the building portfolio was applied to scale the vulnerability analysis from building-level to regional-level, but the method is applicable to smaller communities or to larger scales such as the entire coastline. For each portfolio of building archetypes corresponding to each hurricane-induced hazard [surgewave, surge (static coastal flooding), and wind], the associated

fragility functions are assigned to each building within the community. These building portfolios were mapped to the community using a mapping algorithm. This algorithm is a Python version 3.9.0 code written in a GIS environment to systematically check certain conditions for each building, including building occupancy and other physical characteristics, and then assign the building archetype that satisfies these specific conditions. The proposed methodology was demonstrated at the state level using the US state of North Carolina as an example. Hazard modeling can be based on either a probabilistic model (e.g., the combination of many simulations such as in the development of a 100-year flood map) or a deterministic model (e.g., a single scenario of a historical or design storm). In this study, scenario-based hazard maps developed based on Hurricane Florence in 2018 served as input for the developed community-level multihazard hurricane vulnerability analysis method. Florence was not a particularly severe storm, but did significantly impact North Carolina overall.

Hazard Modeling

The intensities of hurricane-induced hazards vary in time and space. Quantifying the spatiotemporal variation of these hazards requires detailed modeling of these hazards and the interaction between them. The wind field is represented by a data-assimilated

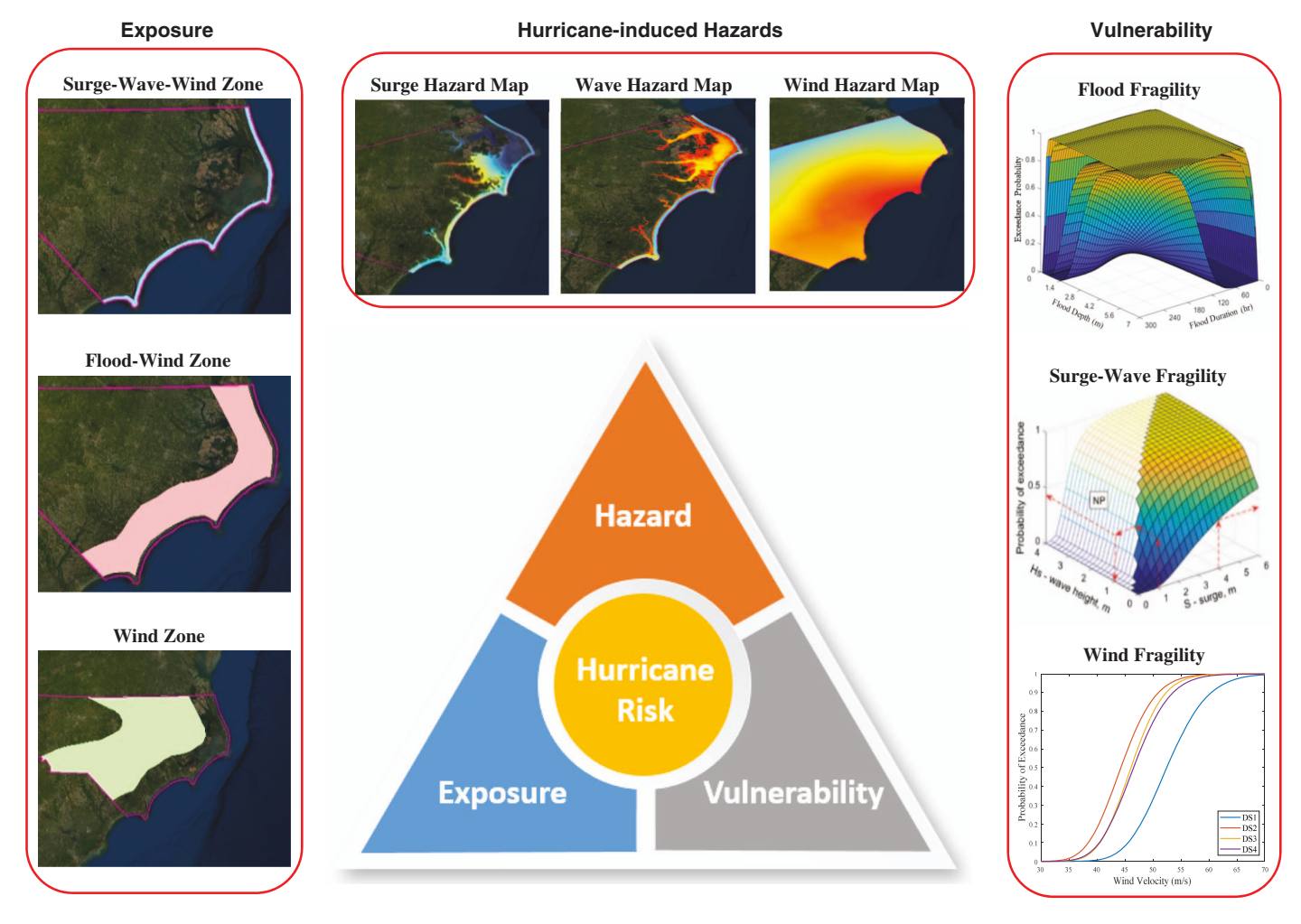


Fig. 1. (Color) Schematic representation of the hurricane risk components and their associated hazard, exposure, and vulnerability models with the example of North Carolina. (Sources: Esri, DigitalGlobe, GeoEye, i-cubed, USDA FSA, USGS, AEX, Getmapping, Aerogrid, IGN, IGP, swisstopo, and the GIS User Community.)

hindcast product which blends inner-core and peripheral wind fields and assimilates in situ, satellite, and aircraft observations (Powell et al. 2010). This product describes the full variation of the wind velocities during the storm, e.g., along the east coast of the US after Hurricane Florence in 2018 (Fig. 2). The wind speed in Fig. 2 is based on the average wind speed in 10.0 min at 10.0 m elevation and was used as input to the surge and wave model described subsequently. This wind speed is based on the full marine-strength wind (open water exposure), but the fragility functions used here are based on the 3-s gust wind speed at 10 m (33 ft) above ground [consistent with ASCE 7-16 (ASCE 2016)] in Exposure C (open terrain). Therefore, the wind hazard map was adjusted from open water exposure to open terrain exposure, and then the wind reference period was adjusted from an average wind speed of 10.0 min to a 3-s gust wind speed. The velocity conversion equation from open water to open terrain and the Durst curve were used to calculate the conversion factor for wind speed as provided by the ASCE 7-16 (ASCE 2016) (conversion factor = 1.24). One of the limitations of the wind hazard map is that the impact of the wind aerodynamics is not included, and a higher-resolution wind hazard map is needed to account for the impact of the surrounding

conditions (e.g., roughness) and the heights and shapes of the buildings on the spatial variation of wind flow and wind speed.

The surge and wave hazard maps were developed using a highresolution simulation with the tightly coupled ADCIRC+SWAN model (Dietrich et al. 2012). The maximum values were used for all hazards, not their time-varying information. These maximum values are not necessarily colocated in time, and the maximum wind can occur at a different time than the maximum surge. The wind hazard was provided on a regular grid with a spacing of 0.25°. The wave and surge hazards were taken from the ADCIRC+SWAN model resolution, which has typical values of 100-200 m in coastal regions but can vary down to 10 m in small-scale channels. The wind, wave, and surge hazards then were mapped onto a raster with a resolution of 10.0 m. Then values were interpolated at the coordinates of each building, including wind speed (meters/second), the surge height measured from the ground (meters), and the significant wave height (meters). In the example provided in this paper, a scenario-based hurricane hazard was utilized for the 2018 Hurricane Florence. Florence was a large storm that caused widespread flooding in multiple cities and counties across the state of North Carolina, resulting in 40 confirmed fatalities, more than 1 million

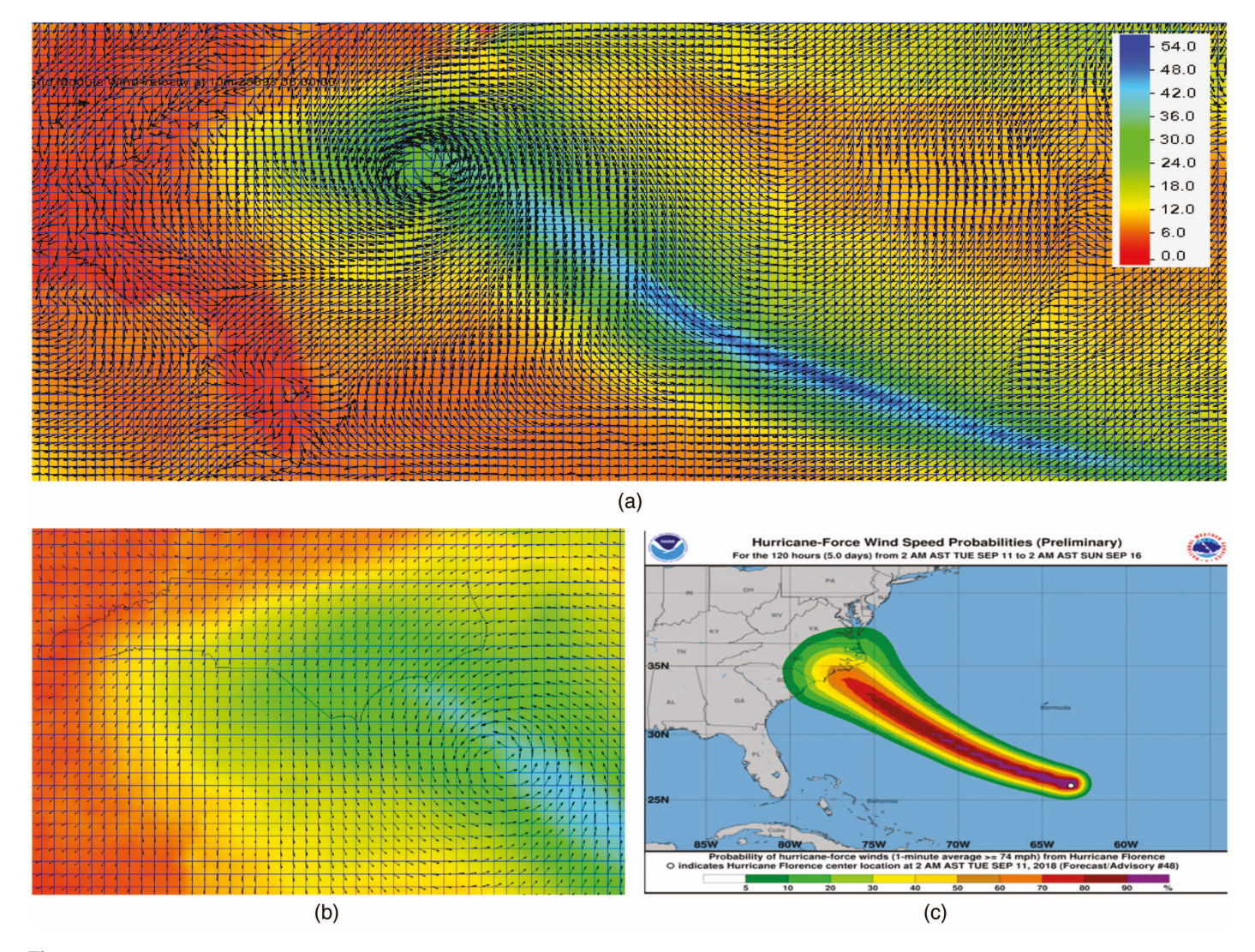


Fig. 2. (Color) Wind simulation based on 2018 Hurricane Florence: (a) maximum wind speed contours and vectors (m/s); (b) close-up view of the maximum winds in North Carolina; and (c) National Weather Service tracking of 2018 Hurricane Florence (reprinted from NOAA 2018, courtesy of NOAA).

people left without power, and an estimated \$17 billion in damage across the state (\$5.6 billion of housing damage, \$5.7 billion of business damage, and \$2.4 billion of agriculture industry losses) (State of North Carolina, Office of the Governor 2018).

Exposure Modeling

As described previously, buildings in a coastal community are exposed to surge, wave, and wind hazards, but with different intensities based on building location and elevation. Therefore, the hazard exposure in coastal communities was divided herein into three zones based on their exposure to the hurricane-induced hazard, namely a surge-wave-wind zone, a surge-wind zone, and a wind zone. Each zone size is proportional to the hazard parameters, including hurricane intensity (e.g., category), wind field size, angle of attack, and the elevation of the coast. The first zone is the surgewave-wind zone, which is approximately the first kilometer of the coast, with a maximum significant wave height close to the coast, which then decreases as the water makes its way inland. The waves are on the top of the surge, which is a large volume of water pushed inland from the ocean by strong hurricane winds. The surge is measured by the surge height, which is the rise in the seawater level above the normal predicted astronomical tide. Waves are measured by the significant wave height, which is the average height of the highest one-third of waves in a storm. The surge and wave action drive multiple hydrodynamic impacts on buildings, thereby jeopardizing the building integrity. The impact of surge accompanied by hurricanes results in immediate loss of building interior contents and some of the nonstructural components, which jeopardizes the serviceability of the impacted buildings. The second zone is the surge-wind zone, which can extend from 3.0 to 30.0 km from the coast, depending on the hurricane category and coast configuration. Beyond this zone, the storm surge starts to weaken and becomes less prevalent, so the third zone includes only wind hazards.

Vulnerability Modeling

Initially, a building-level vulnerability analysis was conducted using fragility functions corresponding to each hurricane-induced hazard within each exposed zone. Fig. 3 is a schematic representation of the different building components, including structural, nonstructural, and interior contents components for a single building archetype example. Each component within the building may be vulnerable to one or multiple hazards at a time, depending on the component type and the hazard characteristics. The resulting damage from some of these hazards to some of the building components is correlated highly, such as the surge-wave impacts on the building structural system. However, some of them are less correlated, such as the surge-wave and wind hazards. In this study, the correlation between surge and wave hazards was considered using multivariate vulnerability functions (e.g., fragility surfaces). Although the correlation between surge-wave and wind hazards was not considered, and their associated damage was calculated from separate vulnerability functions assuming that their maximum intensities do not happen at the same time, the maximum damage state from each vulnerability function was assigned to each corresponding building. Table 1 summarizes the predefined exposure zones in terms of the hazard type and the corresponding vulnerability functions associated with each zone.

In Zone 1, the impact of the surge-wave action on buildings is assumed to be independent of the wind impacts. The surge-wave action is modeled using the surge-wave fragility surfaces developed by Do et al. (2020), whereas the wind action was modeled using the wind fragility functions developed by Memari et al. (2018). This wind fragility function portfolio provides lognormal parameters for wind fragilities with and without tornado factors.

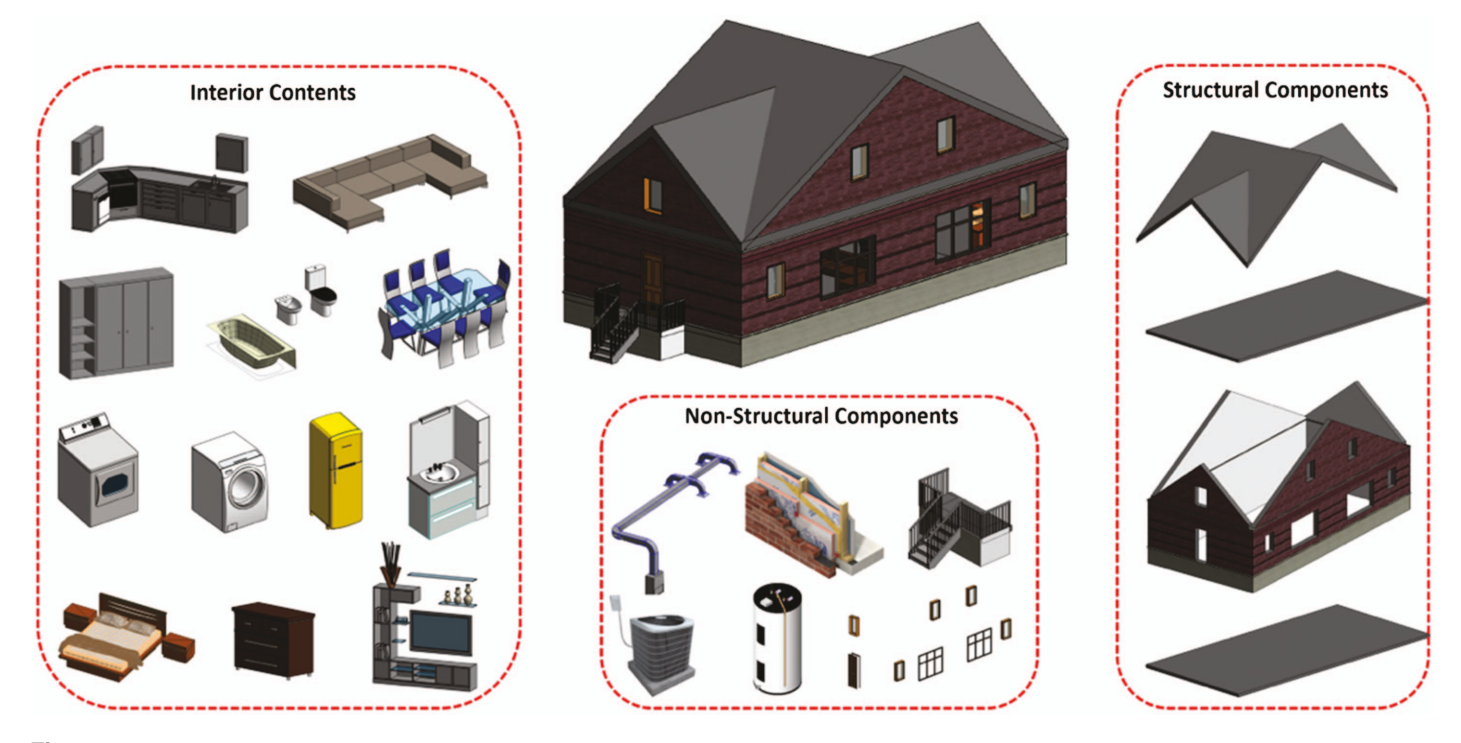


Fig. 3. (Color) Schematic representation showing the different building components including structural and nonstructural components along with interior contents.

Table 1. Hazard types associated with each exposed zone and their corresponding vulnerability functions

					Fragility function	I.
		Hazard type		Structural da	amage	Content damage
Zone	Wave	Surge	Wind	Surge-wave	Wind	Flood
Zone 1	Yes	Yes	Yes	Yes	Yes	Yes
Zone 2	No	Yes	Yes	Yes ^a	Yes	Yes
Zone 3	No	No	Yes	No	Yes	No

^aTwo-dimensional version of surge–wave fragility function is used at significant wave height = 0.

Therefore, in this hurricane study, the wind fragilities used are based on the approach without tornado factors, making them representative of regular wind loading such as that in a hurricane. These wind fragility functions account for the impacts of the external and internal wind pressures after propagating the uncertainties for the different wind factors such as the exposure factor, topographic factor, directionality factor, and the gust factors. However, the factors affecting the pressure equation in ASCE7-16 are not adjusted after the fragility is assigned to a building in the regional level model. This wind portfolio includes 19 building archetypes with different building occupancies that collectively are felt to adequately represent the portfolio of a typical community. These archetypes have different building sizes (e.g., small, medium, and large) and different roof shapes (e.g., hip and gable roofs). However, none of the surge-wave and wind fragility functions used herein accounts for content damage. Therefore, the flood fragility functions developed by Nofal and van de Lindt (2020c) are used to account for contents damage in this zone, i.e., damage due to surge.

In total, three different building archetypes are assigned to each building: an archetype for surge-wave damage to the structural components, an archetype for the wind damage to the structural components, and the third archetype for the surge (e.g., inundation) damage to the interior contents. This is because each of these archetypes is designed such that it includes the necessary parameters associated with each hazard that affects the buildings damage mechanism. For example, the roof shape (e.g., gable or hip roof) is very important in determining the wind damage, but it is not important for flood damage. Therefore there are five different residential building archetypes distinguished by the roof shape. Similarly, the foundation type (e.g., slab-on-grade or crawlspace foundation) is important in determining surge damage, but it is not important for wind damage. Therefore there are four different residential building archetypes distinguished by their foundation type. Fig. 4 is a schematic of the hazard maps (surge, wave, and wind) used to calculate the necessary hazard intensities associated with each fragility function. This was done by extracting the hazard intensity at each building location and using the fragility functions corresponding to each building to calculate the exceedance probability of each damage state. The vulnerability of structural components (e.g., roof, walls, foundation, slabs, and so forth) was derived from the surge-wave fragility surface and the wind fragility curves. The vulnerability of the interior contents and other nonstructural components was calculated from flood fragility functions. This analysis can be performed using two-dimensional (2D) flood depth fragility curves for high-flood duration scenarios or using three-dimensional (3D) flood depth-duration fragility surfaces to include the impact of any specified duration.

Zone 2 is similar to Zone 1 except that it includes no impacts from waves, so the impact of surge hazard only is calculated using the 2D version of the surge—wave fragility surface (at significant wave height = zero), the impact of wind is calculated using the wind

fragility portfolio to account for the structural damage, and the flood fragilities are used to account for contents damage. In Zone 3, buildings are assumed to be vulnerable to wind hazards only, with no vulnerability to surge and/or waves. Therefore, only the wind fragilities are applied to model building vulnerability in Zone 3. Some of these fragility functions are based on a single variable, such as wind fragility (for which wind velocity is the only intensity measure), which is in line with state-of-the-art for those hazards. However, most of the other fragility functions used here are multivariate functions in terms of fragility surfaces. This includes the surge-wave (for which wave height and surge depth are the intensity measures) and the surge fragility (for which flood depth and flood duration are the intensity measures). In this context, both wind fragility functions and surge-wave fragility functions are used to account for structural damage, without including the damage to the building interior contents. The contents damage resulting from static flood fragility functions is based mainly on contents damage from DS0 to DS3, and the structural damage is included separately in DS4 when the structure system deteriorates due to the long duration of flooding, which is the case with urban flooding. Therefore, in this study, DS4 associated with static flooding is excluded because the structural damage resulting from inland flooding has a completely different mechanism from that caused by coastal flooding. Coastal flooding causes gradual structural damage from DS1 to DS4 because of the hydrodynamic impact of the combined surge and waves. Each DS for each hazard is summarized in Table 2 along with their corresponding damage scales. Detailed DS descriptions of each hazard were included in publications corresponding to each fragility function (Do et al. 2020; Memari et al. 2018; Nofal and van de Lindt 2020b).

The community-level hurricane vulnerability analysis then is conducted using the building portfolio concept to model the different building types within a community (Lin and Wang 2016), in which a certain number of archetypes composing a portfolio are used to populate the building stock within a community. The building archetypes within each portfolio were developed such that they were felt to represent the number of different building types needed to accurately represent a community. Each hazard has its own portfolio of building archetypes based on the hazard characteristics and the mechanism through which each hazard causes damage to each building archetype. The building archetypes within each portfolio are assigned to the buildings within a community using a robust mapping algorithm along with GIS tools for spatial analysis. The building data (e.g., Hazus-based building occupancy, number of stories, building area, roof shape, foundation type, and construction material) are used as an input for this algorithm to specify the archetype corresponding to each building within a community. This algorithm is based on a Python function that systematically checks a number of conditions to assign the archetype that matches building characteristics. A sample of the logic of the developed algorithm is given subsequently as an example for identifying the residential wind archetypes using the building occupancy, roof

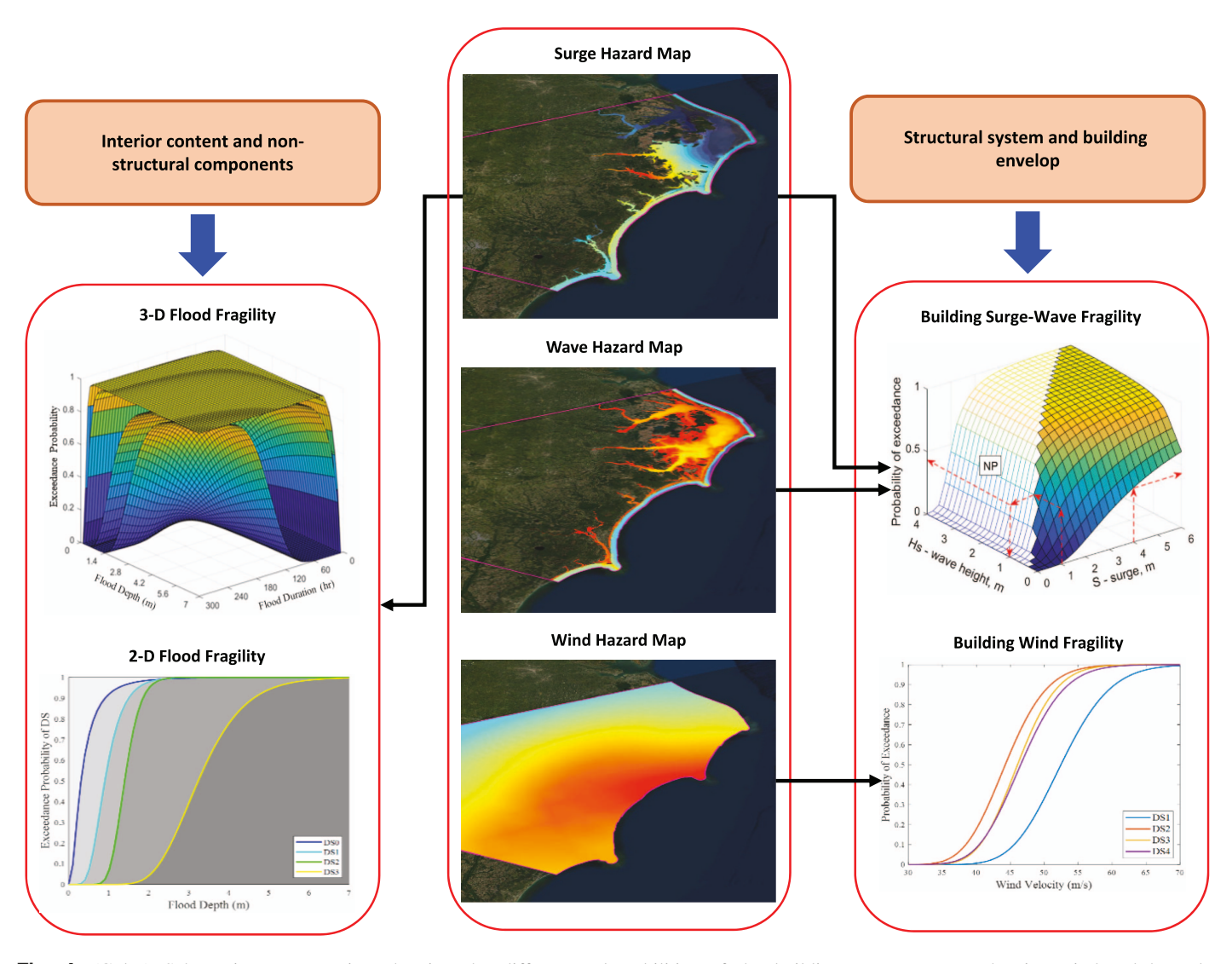


Fig. 4. (Color) Schematic representation showing the different vulnerabilities of the building components to hurricane-induced hazards. (Sources: Esri, DigitalGlobe, GeoEye, i-cubed, USDA FSA, USGS, AEX, Getmapping, Aerogrid, IGN, IGP, swisstopo, and the GIS User Community.)

Table 2. Damage states description for multiple hazards driven by hurricanes and their damage scale

Damage state	Damage scale	Structural damage	Contents damage
DS0	Insignificant	No structural damage	Insignificant damage to components below FFE such as crawlspace items (e.g., insulation, storage, and so forth). Minor damage to garage interiors.
DS1	Slight	Minor damage to the building envelope with damage to ≤15% of roof covering, two or more doors and windows, and ≤25% of exterior wall, and no roof structure damage.	Damage to flooring items including carpets, pads, and baseboards. Air conditioning and other HVAC items are lost if they are not elevated.
DS2	Moderate	Moderate damage to building envelope with damage to ≤50% of roof covering, ≤25% of doors and windows, and ≤50% of exterior wall, and no roof structure damage.	Partial damage to drywall, electrical components, and cabinets. Complete damage to equipment, appliances, and furniture on first floor.
DS3	Extensive	Extensive damage to building envelope with damage to >50% of the roof covering >25% of doors and windows, and ≤75% of exterior wall, and no roof structure damage.	Extensive damage to building interiors including major damage to nonstructural components, drywall, upper cabinets, and lighting fixtures.
DS4	Complete	Complete damage to building envelope along with extensive structure damage to >50% of roof covering, >25% of doors and windows, >75% of exterior wall, and roof structure damage.	Complete damage to interior content and nonstructural components within whole building.

shape, number of stories, and the building area. This function is used in a for-loop to assign an archetype for each building within the community, and returns the archetype number to be used further in the analysis process. A similar function was developed for the other building occupancies and the flood archetypes assignment process. Tables 3 and 4 provide detailed descriptions of the wind and flood archetypes, respectively. For surge and wave hazards, a one-story residential building archetype developed by Do et al. (2020) is used, which allows calculating building damage at different first-floor elevations. Finally, these portfolios were assigned to an example coastal region to illustrate the applicability of the proposed multihazard framework and its scalability to be used at the regional-level. Fig. 5 is a schematic representation of the mapping

Table 3. Description of wind building archetypes

Archetype	Building description
T1	Residential wood building, small rectangular plan, gable roof, one story
T2	Residential wood building, small square plan, gable roof, two stories
Т3	Residential wood building, medium rectangular plan, gable roof, one story
T4	Residential wood building, medium rectangular plan, hip roof, two stories
T5	Residential wood building, large rectangular plan, gable, roof, two stories
T6	Business and retail building (strip mall)
T7	Light industrial building
Т8	Heavy industrial building
Т9	Elementary/middle school (unreinforced masonry)
T10	High school (reinforced masonry)
T11	Fire/police station
T12	Hospital
T13	Community center/church
T14	Government building
T15	Large big-box
T16	Small big-box
T17	Mobile home
T18	Shopping center
T19	Office building

Source: Data from Memari et al. (2018).

Table 4. Description of flood building archetypes

Archetype	Building description
F1	One-story residential building on a crawlspace foundation
F2	One-story residential building on a slab-on-grade foundation
F3	Two-story residential building on a crawlspace foundation
F4	Two-story residential building on a slab-on-grade foundation
F5	Small grocery store/gas station with a convenience store
	(small business)
F6	Super retail building (strip mall)
F7	Small multibusiness building
F8	Super shopping center
F9	Industrial building
F10	One-story school
F11	Two-story school
F12	Hospital
F13	Community center (church)
F14	Office building
F15	Warehouse (small/large box)

Source: Data from Nofal and van de Lindt (2020d).

process with the visualization of a real community and the archetype mapped to this community.

The algorithm to map building archetypes to the buildings within the community is as follows:

```
def Wind_Archetype(occupancy, roof_shp, n_stories, bldg_area): if occupancy = residential and roof_shp = gable and n_stories = 1 and bldg_area <= 116 m<sup>2</sup>
```

return archetype 1

if occupancy = residential and roof_shp = gable and n_stories = 2 and bldg_area \leq 116 m²

return archetype 2

if occupancy = residential and roof_shp = gable and n_stories = 1 and bldg_area $> 116 \text{ m}^2$

return archetype 3

if occupancy = residential and roof_shp = hip and n_stories = 2 return archetype 4

if occupancy = residential and roof_shp = gable and n_stories = 2 and bldg_area $> 116 \text{ m}^2$ return archetype 5

Risk Analysis

The risk analysis necessitates accounting for both hazard and consequences. Building-level and regional-level risk analyses were conducted herein to illustrate the scalability of the proposed methodology. The high-resolution multihazard hurricane risk analysis methodology developed in this study begins with the mapping of each risk component, which includes hazard, exposure, and vulnerability. The flowchart in Fig. 6 shows the logic of the algorithm developed for this method, which starts by overlaying the hazard layers (surge, wave, and wind) with information about the exposed buildings in a GIS environment to relate the spatial location of each building to the spatial variation of the different hazard types across the community. Then the value of each hazard intensity (surge, wave, and wind) corresponding to each building location is calculated. This allows distinguishing each exposure zone associated with each building based on the calculated hazard intensity and consequently performing the corresponding needed vulnerability analyses. Then the new mapping algorithm is applied to map the building archetypes to each building within the community. This also includes mapping the associated vulnerability functions for each portfolio corresponding to each hazard type. This enables the calculation of the exceedance probability of each DS for each building corresponding to each hazard. A detailed damage and loss analysis then is conducted to identify the final DS for each building and the total amount of losses based on its vulnerability to the combinations of hazards induced by the hurricane scenario. Finally, these losses are mapped back to the community to identify the spatial extent and severity of damage induced by hurricanes across the

For building-level analysis, the proposed framework uses five input variables $(x_1, x_2, x_3, x_4, \text{ and } x_5)$ for each building to account for hurricane risk and its associated damage and loss. These variables are the significant wave height, surge depth, building elevation from the ground, maximum wind speed, and flood duration, respectively. For Zone 1, all these variables are used as inputs for three stages of fragility analysis to account for structure and content damage and losses for each building within the community. For Stage 1, the significant wave height, the surge still water depth, and the elevation from the ground are used to account for the structural system exceedance probability of each DS using the multivariate 3D surge—wave fragility function. For loss analysis, the maximum probability of being in each DS corresponding to Stage 1 is calculated and designated DS_SW. For Stage 2, the

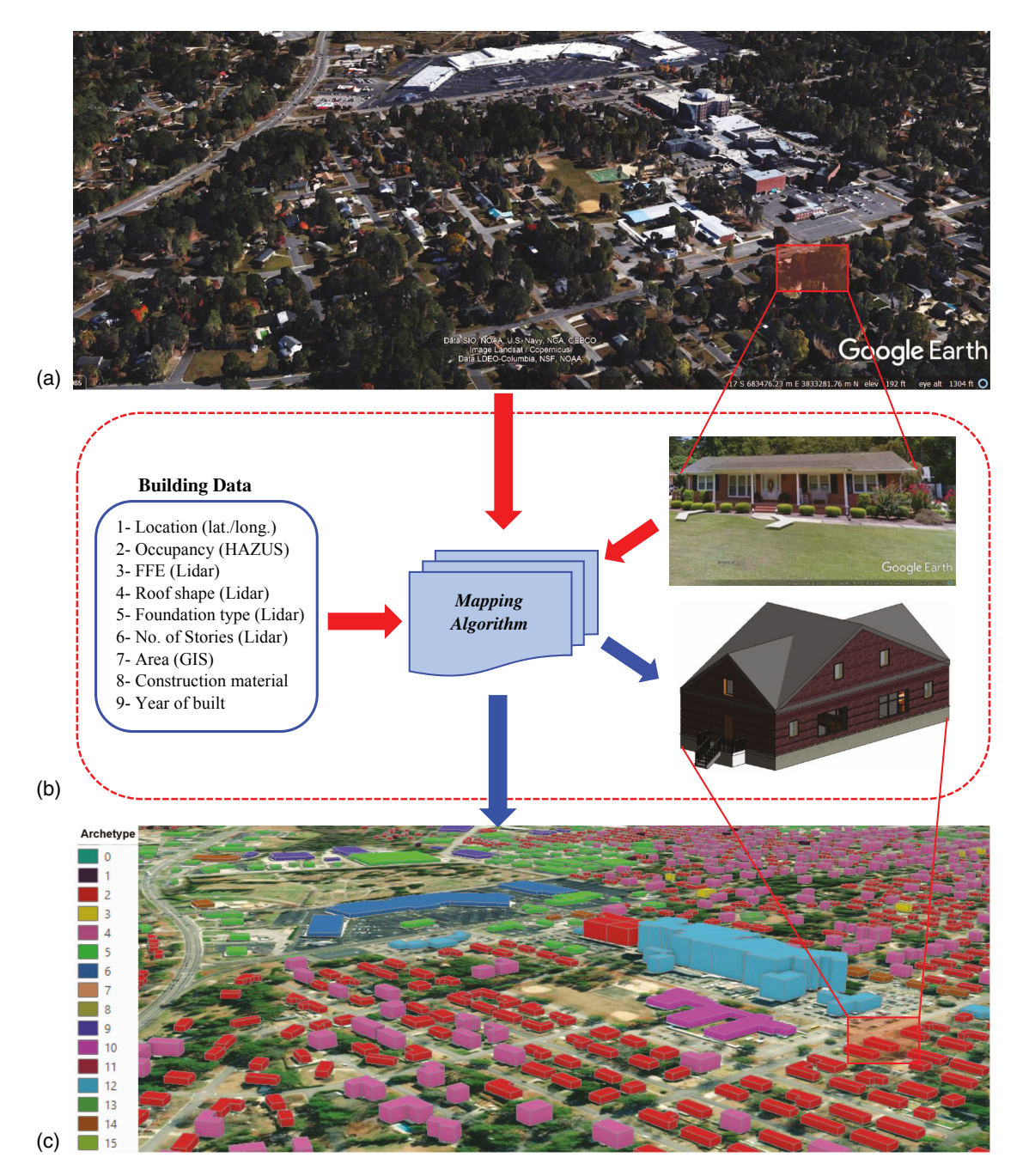


Fig. 5. (Color) Schematic representation showing how a portfolio of builing archetypes is mapped to buildings within a community based on detailed building data: (a) 3D view of the real community (image © Google, Data SIO, NOAA, U.S. Navy, NGA, GEBCO, Image Landsat/Copernicus, Data LDEO-Columbia, NSF, NOAA); (b) mapping algorithm work flow (image © 2021 Google); and (c) 3D view of the mapped community. (Sources: Esri, DigitalGlobe, GeoEye, i-cubed, USDA FSA, USGS, AEX, Getmapping, Aerogrid, IGN, IGP, swisstopo, and the GIS User Community.)

maximum wind speed for each building is used to account for another list of exceedance probabilities for each DS using the wind fragility portfolio, and then the maximum probability of being in each DS corresponding to Stage 2 is calculated and designated DS_W. For Stage 3, flood depth, flood duration, and the building elevation from the ground for each building are used in a 3D multivariate static flood fragility functions to account for contents damage. Then the maximum probability of being in each DS corresponding to Stage 3 is calculated and designated DS_F. For loss and damage analysis, a single DS is assigned to each building based on the maximum DS calculated at each stage (DS_SW, DS_W, and

DS_F) using Eq. (1). The total building loss then is calculated by multiplying the probability of being in each DS by the replacement cost of each DS corresponding to each analysis stage using Eq. (2). The first two terms of the loss functions are associated with the structural damage from surge—wave and wind, and the third term is associated with content damage from flooding. For Zone 2, the same procedures were used, but the 3D surge-wave fragility function is replaced with its 2D version at a significant wave height equal to zero. For Zone 3, Stage 2 only is conducted, which includes only wind damage to the building envelope and structural system, assuming no rainfall intrusion

$$\operatorname{Bldg_DS}(\operatorname{IMs} = x_1 : x_5) = \operatorname{Max} \begin{pmatrix} \operatorname{DS_SW}_{\operatorname{max}} \\ \operatorname{DS_W}_{\operatorname{max}} \\ \operatorname{DS_F}_{\operatorname{max}} \end{pmatrix} \rightarrow \begin{pmatrix} \lim_{i=1}^{i=4} P(\operatorname{DS_SW}_i | \operatorname{IMs}) - P(\operatorname{DS_SW}_{i+1} | \operatorname{IMs}) \\ \lim_{i=1}^{i=4} P(\operatorname{DS_W}_i | \operatorname{IMs}) - P(\operatorname{DS_W}_{i+1} | \operatorname{IMs}) \\ \lim_{i=1}^{i=4} P(\operatorname{DS_W}_i | \operatorname{IMs}) - P(\operatorname{DS_F}_{i+1} | \operatorname{IMs}) \\ \lim_{i=0}^{i=3} P(\operatorname{DS_F}_i | \operatorname{IMs}) - P(\operatorname{DS_F}_{i+1} | \operatorname{IMs}) \end{pmatrix}$$

$$(1)$$

$$L_{f}(IMs = x_{1}:x_{5}) = \sum_{i=1}^{4} [P(DS_SW_{i}|IMs = x_{1}:x_{3}) - P(DS_SW_{i+1}|IM = x_{1}:x_{3})] \times Lr_{s1,i} \times V_{s1}$$

$$+ \sum_{i=1}^{4} [P(DS_W_{i}|IMs = x_{4}) - P(DS_W_{i+1}|IM = x_{4})] \times Lr_{s2,i} \times V_{s2}$$

$$+ \sum_{i=0}^{3} [P(DS_F_{i}|IMs = x_{1},x_{3},x_{5}) - P(DS_F_{i+1}|IM = x_{1},x_{3},x_{5})] \times Lr_{c,i} \times V_{c}$$

$$(2)$$

where x_1 – x_5 = five input variables for damage assessment, namely significant wave height, surge depth, building elevation from ground, maximum wind speed, and flood duration, respectively; Bldg_DS(IMs = x_1 : x_5) = building DS corresponding to five input variables; $P[DS_SW_i|(IM = x_1:x_3)]$ = exceedance probability of DS_SW_i at (IMs = x_1 : x_3) calculated from surge–wave fragility; and $P[DS_SW_{i+1}|(IM = x_1:x_3)]$ = exceedance probability of

DS_SW_{i+1} at (IMs = x_1 : x_3) calculated from surge—wave fragility; $P[DS_-W_i|(IM = x_4)] = exceedance$ probability of DS_ W_i at (IMs = x_4) calculated from wind fragility; $P[DS_-W_{i+1}|(IM = x_4)] = exceedance$ probability of DS_ W_{i+1} at (IMs = x_1, x_2, x_3) calculated from wind fragility; $P[DS_-F_i|(IM = x_1, x_3, x_5)] = exceedance$ probability of DS_ F_i at (IMs = x_1, x_3, x_5) calculated from flood fragility; $P[DS_-F_{i+1}|(IM = x_1, x_3, x_5)] = exceedance$

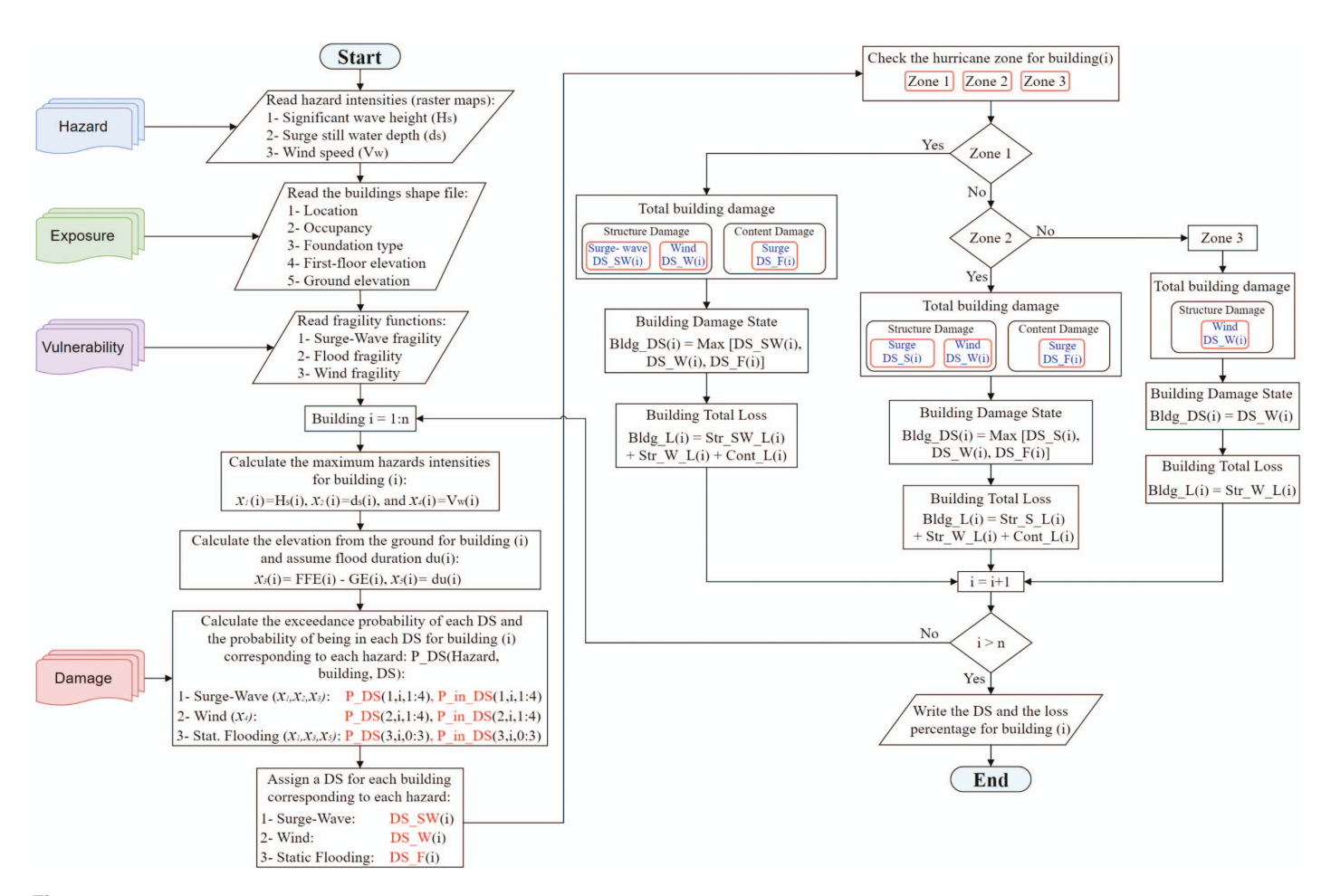


Fig. 6. (Color) Detailed framework for the community-level multihazard hurricane risk assessment model that accounts for building damage and losses.

Table 5. Loss percentage of contents and structure damage for each damage state

Damage					
state	Damage scale	Walls sheathing and framing	Roof sheathing and framing	Decking and foundation	Contents damage
DS0	Insignificant	0.00	0.00	0.00	0.00-0.04
DS1	Slight	0.02-0.25	0.02-0.15	0.02-0.10	0.04-0.20
DS2	Moderate	0.25-0.50	0.15-0.50	0.10-0.50	0.20 - 0.70
DS3	Extensive	0.50-0.75	0.50-0.75	0.50-0.75	0.70 - 1.00
DS4	Complete	0.75–1.00	0.75-1.00	0.75-1.00	1.00

probability of DS_F_{i+1} at $(IMs = x_1, x_2, x_3)$ calculated from flood fragility; L_f $(IMs = x_1:x_5)$ = total building fragility-based losses; $Lr_{s1,i}$ = cumulative replacement cost ratio of structure damage associated with surge and wave loads corresponding to DS_SW_i ; V_{s1} = structure replacement cost associated with surge and wave loads; $Lr_{s2,i}$ = cumulative replacement cost ratio of structure damage associated with wind load corresponding to DS_W_i ; and V_{s2} = structure replacement cost associated with wind loads; $Lr_{c,i}$ = cumulative replacement cost ratio of building content corresponding to DS_F_i ; and V_c = contents replacement cost.

In terms of losses, the total building replacement cost is divided into structure and contents losses. The structure losses are divided further into three parts: walls and framing, roof sheathing and roof framing, and decking and foundation. Table 5 lists the loss percentage ranges associated with each of these divisions corresponding to each DS. These percentages are derived from the DS descriptions given by Do et al. (2020), Memari et al. (2018), and Nofal and van de Lindt (2020b). However, specific loss percentages for each building archetype corresponding to each DS were used herein based on the detailed cost analysis methodology developed by

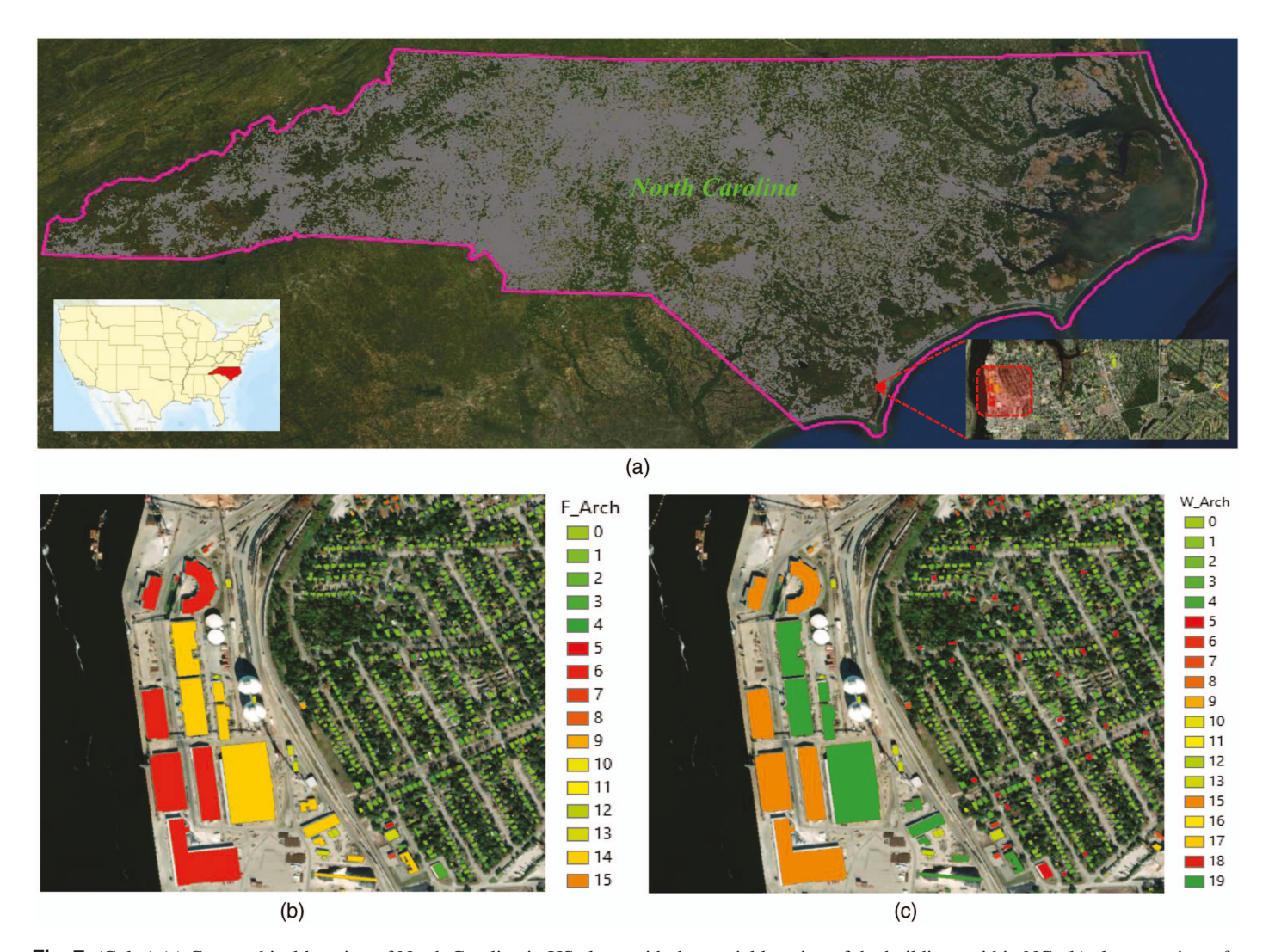


Fig. 7. (Color) (a) Geographical location of North Carolina in US along with the spatial location of the buildings within NC; (b) close-up view of a neighborhood on the bank of the Cape Fear River with color-coded buildings based on the 15 flood archetypes; and (c) close-up view of a neighborhood on the bank of the Cape Fear River with color-coded buildings based on the 19 wind archetypes. (Sources: Esri, DigitalGlobe, GeoEye, i-cubed, USDA FSA, USGS, AEX, Getmapping, Aerogrid, IGN, IGP, swisstopo, and the GIS User Community.)

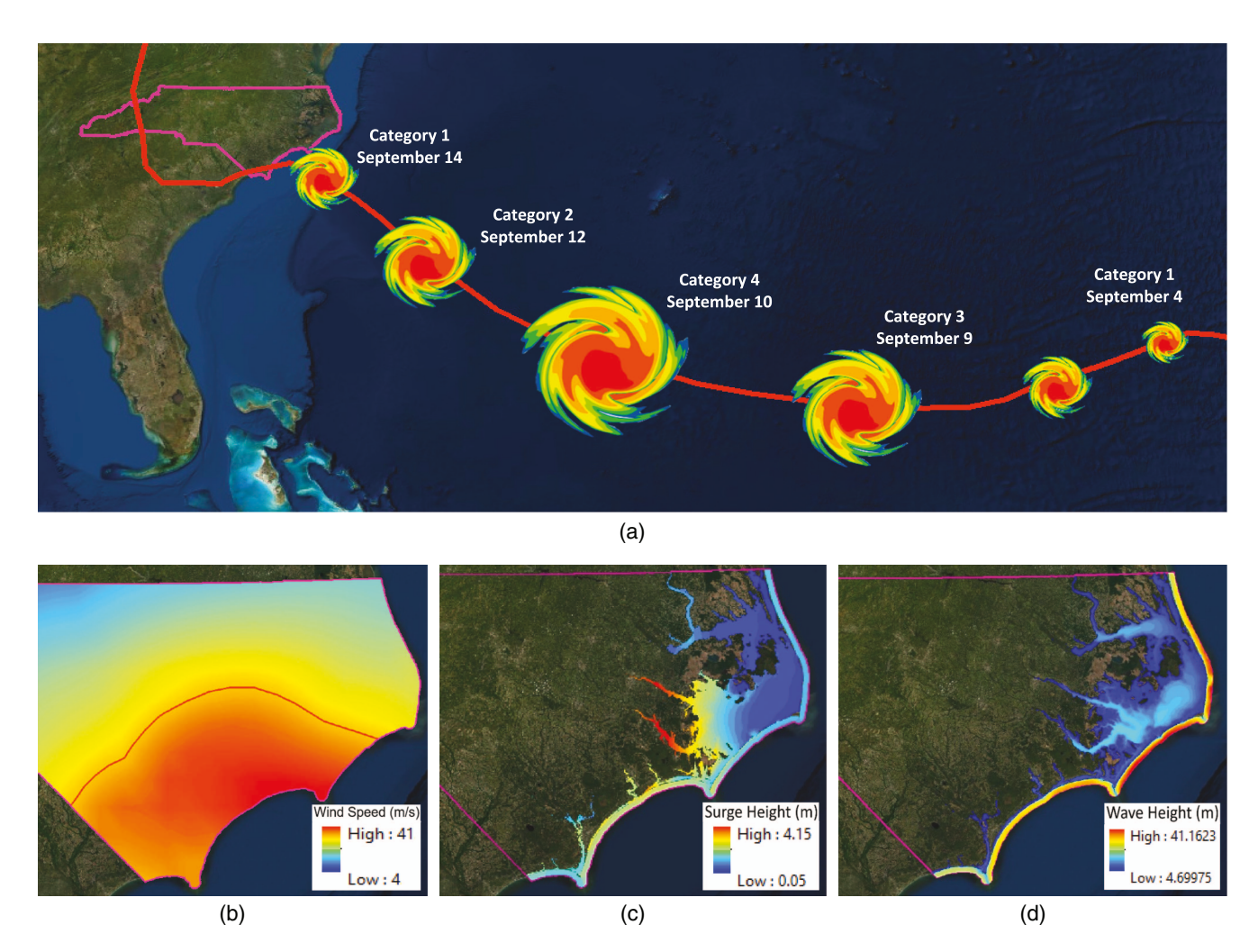


Fig. 8. (Color) Evolution of Hurricane Florence in 2018 along with the resultant hazard maps: (a) evolution of Hurricane Florence in the Atlantic Ocean; (b) wind speed hazard map (m/s); (c) surge height hazard map (m); and (d) significant wave height hazard map (m). (Sources: Esri, DigitalGlobe, GeoEye, i-cubed, USDA FSA, USGS, AEX, Getmapping, Aerogrid, IGN, IGP, swisstopo, and the GIS User Community.)



Fig. 9. (Color) Different exposure zones to hurricane-induced hazards for the state of North Carolina corresponding to 2018 Hurricane Florence. (Sources: Esri, DigitalGlobe, GeoEye, i-cubed, USDA FSA, USGS, AEX, Getmapping, Aerogrid, IGN, IGP, swisstopo, and the GIS User Community.)

Nofal and van de Lindt (2020b). Roof losses are calculated using the wind DS because roof damage is assumed to occur from wind loads, whereas floor system and foundation losses are calculated using surge—wave DS because most of their damage results from surge and waves. Walls and framing typically are impacted by both wind and surge—wave loads. Therefore, the higher DS from both wind and surge—wave is used to account for walls and framing losses. Finally, contents damage is calculated using the static flood fragility.

Illustrative Example: State of North Carolina

The state of North Carolina, located on the east coast of the United States (Fig. 7), is a large coastal state in terms of area and population (29th and 9th, respectively, of 50 US states). The population of North Carolina according to the 2019 state census data was 10.49 million (US Census Bureau 2019), and the state had more than 5 million buildings, ranging from residential to commercial and industrial buildings, as well as social institutions such as schools and hospitals. North Carolina has a long history of damage and loss from coastal hazards, including hurricanes, over the last several decades (e.g., Hurricane Floyd in 1999; Hurricane Matthew in 2016, and Hurricane Florence in 2018). Hence, it was selected as

Table 6. Number of buildings exposed to hazards induced by Hurricane Florence (2018)

Hazard type	Hazard intensity	No. of buildings
Wind (m/s)	$31.0 \le V_w < 34.0$	315,706
	$34.0 \le V_w < 37.0$	320,552
	$37.0 \le V_w < 40.0$	208,543
	$40.0 \le V_w$	0
Surge (m)	$0.0 \le d_s < 1.0$	2,434
	$1.0 \le d_s < 2.0$	8,391
	$2.0 \le d_s < 3.0$	4,763
	$3.0 \le d_s$	4
Wave (m)	$0.0 \le H_s < 0.5$	9,648
	$0.5 \le H_s < 1.0$	5,080
	$1.0 \le H_s < 2.0$	152
	$2.0 \le H_s$	0

the illustrative example for the proposed multihazard hurricane risk analysis approach presented in this paper, using Hurricane Florence from 2018. Full buildings data for North Carolina are published on the state's spatial data download website (State of North Carolina 2019). These data include each building location, Hazus-based occupancy, year built, first-floor elevation (FFE), number of stories, foundation type, roof shape, and market value. The spatial location of each building within North Carolina is indicated in gray in Fig. 7 (a). Close-up views of one of the coastal areas in North Carolina are

shown in Figs. 7(b and c) along with color-coded buildings based on the flood and wind archetype portfolio, respectively.

Results

Hazard Analysis Results

Hurricane Florence started as a Category 1 storm on September 4, 2018 in the Atlantic Ocean and intensified to a Category 4 storm on September 10, then weakened and made landfall as a Category 1 storm in the US just south of Wrightsville Beach, North Carolina [Fig. 8(a)]. A hazard map for each of the hurricane-induced hazards from Hurricane Florence was developed for the state of North Carolina, including surge, wave, and wind [Figs. 8(b-d)]. The wind hazard map is based on the maximum wind speed for North Carolina in terms of the 3-s guest wind speed in open terrain from 4.0 to 41.0 m/s (9.0 to 91.0 mi/h) [Fig. 8(b)]. However, only buildings experiencing wind speeds exceeding 31.0 m/s (61.0 mph) were considered in this study, because it is the lowest wind speed that typically would cause damage based on a 50% exceedance probability of DS1 for the residential wind fragilities (Memari et al. 2018). Therefore, the zone with wind speeds exceeding 31.0 m/s (70.0 mph) is distinguished by the red boundary line in Fig. 8(b). The peak surge height for the flooded areas throughout North Carolina in this example is shown in Fig. 8(c), not including



Fig. 10. (Color) Example of the archetype assignment to each building within the community based on each mapped building archetype: (a) Google Earth close-up view of Carolina Beach, North Carolina (image © Google, Image Landsat/Copernicus); (b) color-coded buildings based on the 15 flood archetypes; and (c) color-coded buildings based on the 19 wind archetypes. (Sources: Esri, DigitalGlobe, GeoEye, i-cubed, USDA FSA, USGS, AEX, Getmapping, Aerogrid, IGN, IGP, swisstopo, and the GIS User Community.)

additional flooding resulting from the rainfall-runoff. Fig. 8(d) shows the wave hazard map based on the significant wave height.

Exposure Analysis Results

The building spatial data was overlaid with the hazard maps to identify the exposed buildings and their corresponding hazard intensities. The entire state of North Carolina was exposed to wind hazard from Hurricane Florence in 2018, but with different intensities. Therefore, as mentioned previously to reduce the number of buildings to be analyzed, a wind speed threshold of 31.0 m/s (70.0 mph) was set to exclude any building experiencing wind speeds less than this threshold. For the surge and wave hazard, all buildings that were exposed to either surge or combined surge and wave were included in the analysis. Fig. 9 shows the different exposure zones within the state of North Carolina, which are colorbased on the types of hazards within each zone. Creating this wind threshold increased the number of exposed zone types to include the wind zone (blue), flood zone (yellow), surge-wave zone (orange), surge-wind zone (green), and surge-wave-wind zone (purple). The two new zones—the surge zone and the surge-wave zone-include wind hazard, but the wind speed was less than

the 31.0 m/s (70.0 mph) threshold, which was assumed to be insufficient to cause any wind-related damage. The exposure analysis results showed that 845,067 buildings were exposed to a wind speed of more than 31.0 m/s (Fig. 9). These included the vast majority, 834,595 buildings, exposed to wind hazard only (based on the used wind speed threshold); 6,741 buildings exposed to combined surge and wind; and 3,465 buildings exposed to combined surge, waves, and wind. The exposure analysis results showed that another 3,336 buildings were exposed to surge only, and 2,050 buildings were exposed to combined surge and wave. Table 6 summarizes the number of buildings exposed to the hazard intensity ranges.

Vulnerability Analysis Results

There are more than 5 million buildings in the state of North Carolina, but the vulnerability analysis included only the 857,046 buildings deemed to be exposed to hurricane-induced hazards. The building archetypes corresponding to each hazard were assigned to the exposed buildings only, and the other buildings were removed from the analysis. Then a fragility function corresponding to each building archetype associated with each hazard type was assigned



Fig. 11. (Color) Surge hazard map overlaid with a part of the community model for Carolina Beach (coastal community in North Carolina): (a) real community; and (b) mapped community with the surge hazard map. (Sources: Esri, DigitalGlobe, GeoEye, i-cubed, USDA FSA, USGS, AEX, Getmapping, Aerogrid, IGN, IGP, swisstopo, and the GIS User Community.)

Table 7. Damage state exceedance probability corresponding to each hurricane-induced hazard for exposed buildings on coastal line of North Carolina

			No. of	buildings (total=8	357,046)	
Hazard type	Exceedance probability of DS (fragility)	DS0	DS1	DS2	DS3	DS4
Surge-wave	P_DS = 0%	_	849,396	850,150	852,389	853,930
-	$0\% < P_DS < 20\%$	_	4,342	3,781	2,459	1,575
	$20\% < P_{-}DS < 40\%$	_	568	596	956	899
	$40\% < P_{-}DS < 60\%$	_	666	584	622	151
	$60\% < P_DS < 80\%$	_	912	941	203	126
	80% < P_DS < 100%	_	1,162	994	417	365
Flood	$P_DS = 0\%$	850,377	846,895	847,913	851,860	_
11004	$0\% < P_DS < 20\%$	179	546	856	2,801	_
	$20\% < P_{-}DS < 40\%$	108	426	491	1,239	_
	$40\% < P_{-}DS < 60\%$	149	501	680	541	_
	$60\% < P_{-}DS < 80\%$	421	555	1,039	359	_
	80% < P_DS < 100%	5,812	8,123	6,067	246	_
Wind	$P_{\rm DS}=0\%$	_	512,983	365,893	669,698	770,389
	$0\% < P_DS < 20\%$	_	115,495	438,251	187,348	86,657
	$20\% < P_{-}DS < 40\%$	_	51,475	35,184	0	0
	$40\% < P_{-}DS < 60\%$	_	28,325	14,768	0	0
	$60\% < P_{-}DS < 80\%$	_	81,910	2,916	0	0
	80% < P_DS < 100%	_	66,858	34	0	0

to each exposed building using the mapping algorithm. Fig. 10 shows color-coded maps for Carolina Beach (a coastal community in North Carolina) based on the building archetypes associated with each hazard type. The digital elevation map (DEM) of the study area was used to extract the ground elevation (GE) of each building within the exposed area. The GE was subtracted from the FFE to account for the absolute elevation from the ground for each building to be used in the surge—wave and flood fragility functions.

Risk Analysis Results

The hazard layer was overlaid with the mapped community model to extract the value of the hazard intensity at each exposed building (Fig. 11) for an example part of the coastline of North Carolina (Carolina Beach). Then a damage and loss analysis algorithm based on the flowchart in Fig. 6 was developed to read the hazard, exposure, and vulnerability of each building within the illustrative example community. The amount of damage and loss for the structural system and interior contents for each building was calculated in terms of the exceedance probability of each DS corresponding to each hazard (surge, wave, and wind). An extreme flood duration of 10 days was assumed in this analysis, but the model can incorporate any flood duration desired. This duration simply damages any components within the building models that otherwise would be able to be dried or salvaged, thereby providing an upper bound on damage from a duration perspective (van de Lindt and Taggart 2009; Nofal et al. 2020; Taggart and van de Lindt 2009). Table 7 summarizes the community-level risk analysis by dividing the probability of exceeding each DS corresponding to each hazard into six ranges

Table 8. Assigned damage states corresponding to each hurricane-induced hazard for exposed buildings on coastal line of North Carolina based on Hurricane Florence (2018)

	Number of buildings (total = 857,046)				
Hazard type	DS0	DS1	DS2	DS3	DS4
Surge-wave	855,382	0	941	3	720
Flood	848,150	1,167	6,758	971	_
Wind	695,237	150,333	11,476	0	0
Multihazard	686,990	150,835	17,616	885	720

and providing the number of buildings within each range. For example, the analysis results in Table 7 in the DS3 column and the last row of flood hazard show that 246 buildings had more than an 80% exceedance probability of DS3 corresponding to flood hazard (inundation), which was used to account for the contents damage. However, 417 buildings had more than an 80% exceedance probability of DS3 corresponding to surge—wave hazard, which was used to account for structural damage. There were 34 buildings with more than an 80% exceedance probability of DS2 corresponding to wind hazard, which also was used to account for structural damage. Finally, each building was assigned a DS based on the maximum probability of being in that DS corresponding to each hazard. Table 8 summarizes the number of buildings within each DS associated with each hazard along with their final DS assignment based on the maximum DS from surge-wave, wind, and flood.

The final hurricane risk analysis showed that 857,046 buildings were exposed to the multiple hazards induced by Hurricane Florence in 2018 including surge, wave, and wind. Of those, the analysis results showed that 686,990 buildings were designated DS0, which means that they did not encounter any damage from surge, wave, or wind. However, 170,056 buildings received some level of damage ranging from DS1 to DS4 (Table 7, last row). The content and structural damage for each building were calculated to account for the total building losses. Table 8 provides six loss ranges and the number of buildings within each range. The contents losses in Table 9 were calculated as a percentage of the total value of the contents, not the total building value. Similarly, the structural

Table 9. Calculated losses for impacted buildings in North Carolina in terms of structural, contents, and total losses based on Hurricane Florence (2018)

	No. of	buildings (total = 857	,046)
Loss (%)	L_Content	L_Structure	L_total
L=0	846,442	693,580	685,514
0 < L < 20	2,314	134,957	163,695
20 < L < 40	1,644	27,242	3,360
40 < L < 60	3,693	752	3,385
60 < L < 80	2,198	357	983
80 < L < 100	755	158	109

losses were calculated as a percentage of the total value of the building structural system. area total of 686,990 buildings were designated DS0, but the number of buildings with zero losses was 685,514, which means that 1,476 buildings were designated DS0 but had losses greater than zero. These 1,476 buildings had crawlspace foundations (Archetypes F1 and F3) and experienced flood damage to components below FFE and insignificant contents losses (0%–4%).

Although some of the buildings that were exposed to surge wave hazard also were exposed to wind hazard, the wind speed was not high enough to cause damage to many of these buildings. Therefore, only a few buildings had structural damage resulting from both wind and surge—wave at the same time. Furthermore, the DS of the buildings that were damaged by wind did not exceed DS2, because the maximum wind speed during Hurricane Florence at landfall was only 41.0 m/s. Fig. 12(a) shows the spatial location of the investigated 857,046 buildings investigated in this example. Fig. 12(c) shows a close-up view of one of the locations in which buildings were damaged by wind, color-coded based on the wind DS. Fig. 12(b) shows a close-up view of the area around the

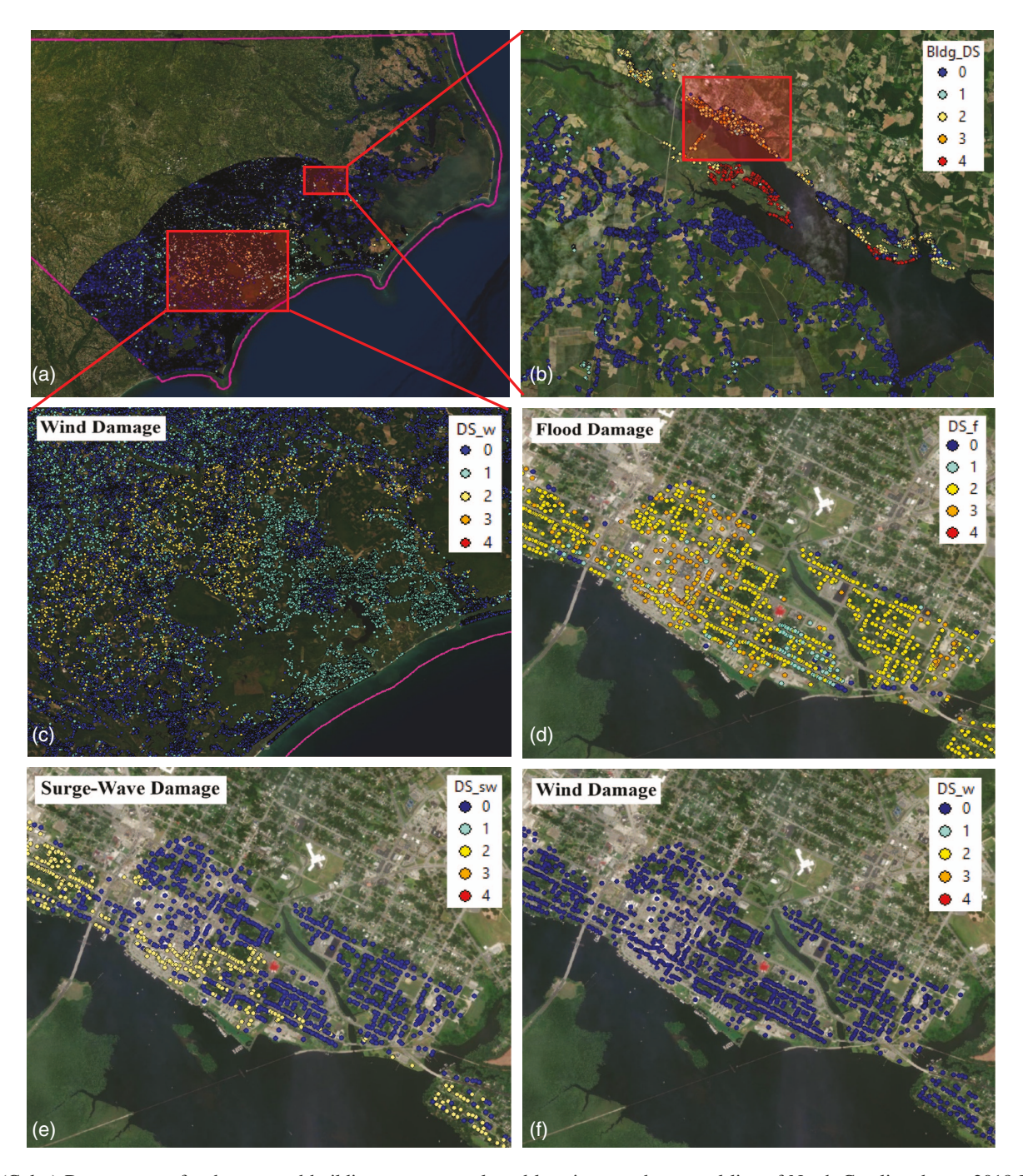


Fig. 12. (Color) Damage state for the exposed buildings on some selected locations on the coastal line of North Carolina due to 2018 Hurricane Florence: (a) exposed building locations; (b) close-up view of the east bank of the Pamlico River; (c) close-up view of the wind-impacted locations; (d) color-coded buildings based on contents damage; (e) color-coded buildings based on structural damage; and (f) color-coded buildings based on total damage. (Sources: Esri, DigitalGlobe, GeoEye, i-cubed, USDA FSA, USGS, AEX, Getmapping, Aerogrid, IGN, IGP, swisstopo, and the GIS User Community.)

Pamlico River, which was one of the locations severely impacted by surge—wave hazard. The surge height simulation in this area ranged from 2.25 to 2.65 m, and the simulated significant wave height ranged from 0.5 to 0.75 m. The USGS sensor in this area recorded a high watermark of 2.3 m (7.5 ft) (Stewart and Berg 2019), which suggests that the simulated surge height had reasonable agreement with the field-measured data.

Figs. 12(d-f) show a closer view of Washington, North Carolina, located on the east bank of the Pamlico River, with the impacted buildings color-coded based on their contents, structural, and total damage, respectively, in terms of the DS assigned to each building. The risk analysis of the buildings vulnerable to the combined storm surge and waves revealed that although many buildings were not damaged structurally (DS0) [Fig. 12(e)], some had slight to complete contents damage (DS1-DS3) [Fig. 12(d)] due to flood inundation from the hurricane storm surge. This affected the final DS assigned to each of these buildings [Fig. 12(f)], which were based on the maximum DS from contents and structural damage. Additionally, the analysis results showed that some buildings may have lower DS/loss than surrounding buildings that had high DS/ loss [Fig. 12(d)]. This can be explained by the value of the five input variables used to assess the building damage (x_1-x_5) . For example, these buildings likely were elevated above ground level (e.g., x_3 was high) and the surrounding buildings were not elevated. Another reason is that the hazard intensity at the location of these buildings was lower than that of the surrounding buildings because of the way the hazard hit that location or because of the topography of the location, which altered the values of the other inputs (e.g., x_1 and x_2). The structural and contents losses corresponding to each building were calculated using Eq. (2). Fig. 13 shows a close-up view of Washington, North Carolina with buildings color-coded based on their losses as a percentage of the replacement cost corresponding to each building. Fig. 13(a) shows the contents loss as a percentage of the market value of the contents, and Fig. 13(b) shows the structural losses as a percentage of the market value of the structural system. The loss analysis also showed that a large number of buildings had zero structural losses (blue circles) but had contents losses up to 80% (red circles). This is reflected in the final total building losses [Fig. 13(c)]. The loss analysis results were consistent with the damage analysis results [Fig. 13(d)].

Computational Efficiency

Different types of analyses were conducted in this study, ranging from hazard, exposure, and vulnerability analyses to risk analysis. For the hazard analysis, the high-fidelity predictions for storm winds, waves, and coastal flooding also had a high computational cost. The surge and wave hazard maps were developed using a high-resolution simulation with the tightly coupled ADCIRC + SWAN model (Dietrich et al. 2012), which is highly scalable to thousands of computational cores (Dietrich et al. 2012; Tanaka et al. 2011). A scenario-based hazard scenario was used in this study because the damage/loss assessment does not need to be developed in real-time, so it can rely on the highest-fidelity predictions of winds, waves, and coastal flooding. The other analyses

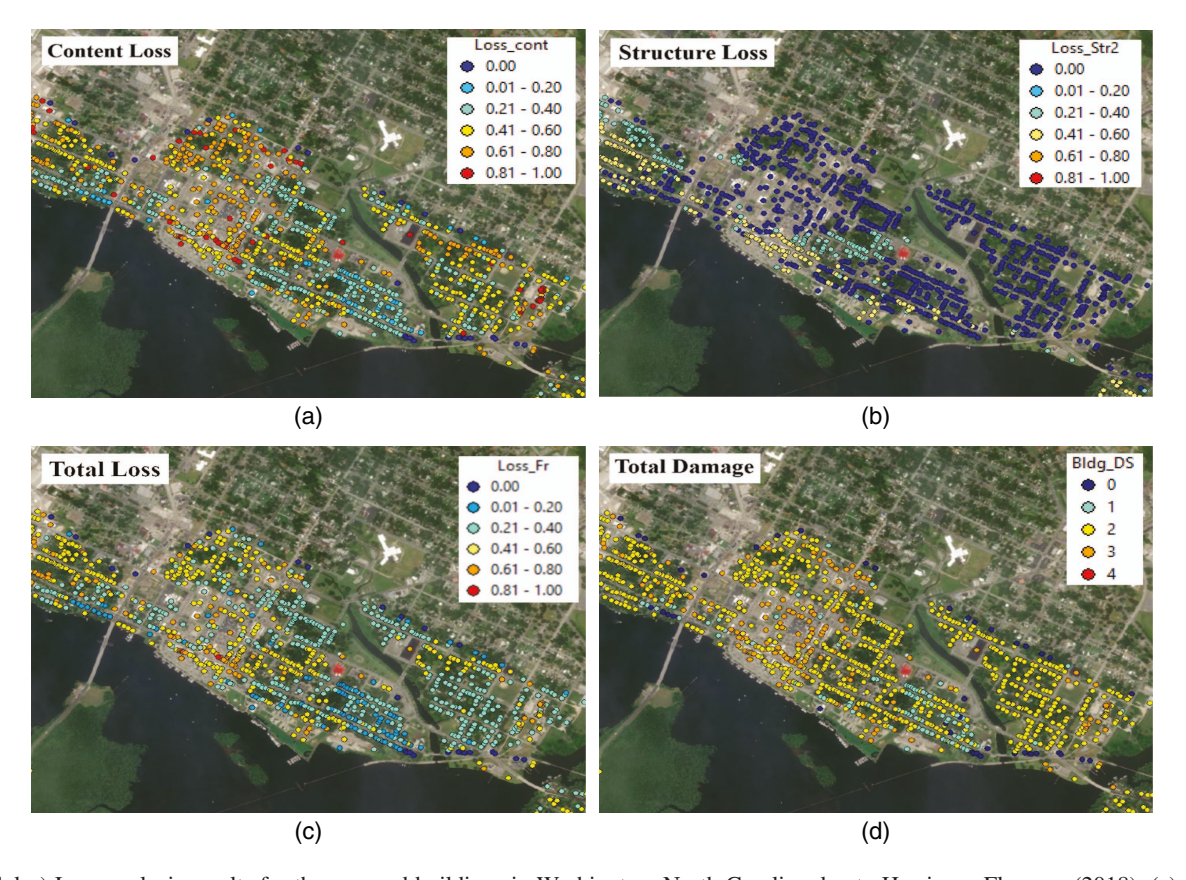


Fig. 13. (Color) Loss analysis results for the exposed buildings in Washington, North Carolina due to Hurricane Florence (2018): (a) color-coded buildings based on contents losses; (b) color-coded buildings based on structural losses; (c) color-coded buildings based on total losses; and (d) color-coded buildings based on building damage. (Sources: Esri, DigitalGlobe, GeoEye, i-cubed, USDA FSA, USGS, AEX, Getmapping, Aerogrid, IGN, IGP, swisstopo, and the GIS User Community.)

were conducted using different algorithms that were coded using MATLAB verion R2020b and Python version 3.9.0. A desktop computer with 16 cores a 3.4 GHz CPU, 128 GB RAM, and a 64-bit Windows 10 operating system was used to develop and run these algorithms. The archetype mapping algorithm running time varies depending on the number of checks (if-statement) associated with each building archetype. In this study, specifically, it took 2-4 min to run the mapping Python code for the 857,000 investigated buildings. The risk analysis algorithm was conducted using a single MATLAB code that reads the buildings shapefiles, assigns fragilities, and calculates damage/loss. This algorithm takes 20-40 min to generate results depending on the number of hazards to which each building is exposed, i.e., wind, wave, and/or surge. The more hazards to which these buildings are exposed, the more running time will be required to calculate their associated damage/ loss. Most of the buildings investigated (98.7%) were exposed to wind hazards only, and the others (1.3%) were exposed to combined hazards, which made the analysis faster. However, it took an additional 2 h to write the analysis results in the original building shapefile to perform further spatial analyses in GIS.

Summary and Conclusion

A high-fidelity (individual buildings used in the calculations) multihazard hurricane risk analysis method was developed to account for large-scale impacts of multiple loadings induced by hurricanes. The concept of combining building portfolios from different hazards was introduced to model hurricane vulnerability at large spatial scales. The combined impacts of surge, wave, and wind on the structural system and interior contents were the novel focus of this study. Specifically, portfolios of building archetypes corresponding to each of these hazards were used and mapped to the buildings within a large region using a mapping algorithm. Then building-level damage was calculated using fragility curves/ surfaces corresponding to each hazard. The structural damage was calculated using the surge-wave and wind fragility functions and the content damage was calculated using surge fragility functions. For the first time, five input variables were used as input for these fragility functions, namely the significant wave height, surge still water depth, building elevation from the ground, maximum wind speed, and flood duration. Losses then were calculated by multiplying the probability of being in each DS by the replacement cost of each DS corresponding to each hazard. The regionallevel hurricane-induced losses then were calculated using North Carolina and the 2018 landfall for Hurricane Florence as an illustrative example. An algorithm was developed to predict the damage and loss for each vulnerable building on the entire North Carolina coast.

The methodology summarized herein underscores that multihazard analysis can provide a robust estimation for both building-level and large spatial analysis. It emphasizes the impact of including the contents damage explicitly resulting from inundation driven by storm surge. Therefore, combining the structural and contents damage can provide a better estimate of the final damage/loss, as well as a better opportunity to investigate the impact of the different mitigation measures at the building level. The scalability of the methodology enables large-scale hurricane damage assessment with detailed quantification of the loadings and their associated impacts on both the structural system and the interior contents. Finally, this type of high-resolution analysis will allow better risk-informed decisions for potential novel investment mechanisms, which ultimately enhances community resilience to hurricane-induced hazards for coastal communities.

Data Availability Statement

Some or all data, models, or codes that support the findings of this study are available from the corresponding author upon reasonable request.

Acknowledgments

This research was a combination of work from two projects, including the National Science Foundation (NSF) Coastlines and People program under Grant No. 1940119, and that support is gratefully acknowledged. The views and opinions expressed in this paper are those of the authors and do not necessarily represent the views of the NSF. The surge/wave fragility development and ADCIRC simulations were funded by the DHS Coastal Center of Excellence through subcontracts from the University of North Carolina at Chapel Hill to Colorado State University and North Carolina State University, respectively.

References

- Abdelhady, A. U., S. M. J. Spence, and J. McCormick. 2018. "Realizing hurricane resilient communities through distributed computing." In *Routledge handbook of sustainable and resilient infrastructure*, 134–151. London: Routledge.
- Abdelhady, A. U., S. M. J. Spence, and J. McCormick. 2020. "A framework for the probabilistic quantification of the resilience of communities to hurricane winds." *J. Wind Eng. Ind. Aerodyn.* 206 (Nov): 104376. https://doi.org/10.1016/j.jweia.2020.104376.
- Aghababaei, M., M. Koliou, and S. G. Paal. 2018. "Performance assessment of building infrastructure impacted by the 2017 Hurricane Harvey in the Port Aransas region." *J. Perform. Constr. Facil.* 32 (5): 4018069. https://doi.org/10.1061/(ASCE)CF.1943-5509.0001215.
- ASCE. 2016. Minimum design loads and associated criteria for buildings and other structures. ASCE 7-16. Reston, VA: ASCE.
- Baradaranshoraka, M., J.-P. Pinelli, K. Gurley, X. Peng, and M. Zhao. 2017. "Hurricane wind versus storm surge damage in the context of a risk prediction model." *J. Struct. Eng.* 143 (9): 4017103. https://doi.org/10.1061/(ASCE)ST.1943-541X.0001824.
- Barbato, M., F. Petrini, V. U. Unnikrishnan, and M. Ciampoli. 2013. "Performance-based hurricane engineering (PBHE) framework." *Struct. Saf.* 45 (Nov): 24–35. https://doi.org/10.1016/j.strusafe.2013.07.002.
- Bushra, N., J. C. Trepanier, and R. V. Rohli. 2019. "Joint probability risk modelling of storm surge and cyclone wind along the coast of Bay of Bengal using a statistical copula." *Int. J. Climatol.* 39 (11): 4206–4217. https://doi.org/10.1002/joc.6068.
- Chen, S.-C., M. Chen, N. Zhao, S. Hamid, K. Chatterjee, and M. Armella. 2009. "Florida public hurricane loss model: Research in multidisciplinary system integration assisting government policy making." Gov. Inf. Q. 26 (2): 285–294. https://doi.org/10.1016/j.giq.2008.12 .004.
- Chung Yau, S., N. Lin, and E. Vanmarcke. 2011. "Hurricane damage and loss estimation using an integrated vulnerability model." *Nat. Hazards Rev.* 12 (4): 184–189. https://doi.org/10.1061/(ASCE)NH.1527-6996.0000035.
- Dietrich, J. C., S. Tanaka, J. J. Westerink, C. N. Dawson, R. A. Luettich Jr.,
 M. Zijlema, L. H. Holthuijsen, J. M. Smith, L. G. Westerink, and
 H. J. Westerink. 2012. "Performance of the unstructured-mesh,
 SWAN+ADCIRC model in computing hurricane waves and surge."
 J. Sci. Comput. 52 (2): 468–497. https://doi.org/10.1007/s10915-011-9555-6.
- Dietrich, J. C., M. Zijlema, J. J. Westerink, L. H. Holthuijsen, C. Dawson, R. A. Luettich Jr., R. E. Jensen, J. M. Smith, G. S. Stelling, and G. W. Stone. 2011. "Modeling hurricane waves and storm surge using integrally-coupled, scalable computations." *Coastal Eng.* 58 (1): 45–65. https://doi.org/10.1016/j.coastaleng.2010.08.001.

- Ding, Y., Y. Zhang, Y. Jia, and M. S. Altinakar. 2016. "Hindcasting of wind, storm surge, and waves from Hurricane Sandy (2012) using an integrated coastal and ocean process model." In *Proc.*, World Environmental and Water Resources Congress, 130–139. Reston, VA: ASCE. https://doi.org/10.1061/9780784479872.014.
- Do, T. Q., J. W. van de Lindt, and D. T. Cox. 2020. "Hurricane surge-wave building fragility methodology for use in damage, loss, and resilience analysis." *J. Struct. Eng.* 146 (1): 4019177. https://doi.org/10.1061/(ASCE)ST.1943-541X.0002472.
- Ellingwood, B. R., D. V. Rosowsky, Y. Li, and J. H. Kim. 2004. "Fragility assessment of light-frame wood construction subjected to wind and earthquake hazards." *J. Struct. Eng.* 130 (12): 1921–1930. https://doi.org/10.1061/(ASCE)0733-9445(2004)130:12(1921).
- FEMA. 2003. Multi-hazard loss estimation methodology: Hurricane model: Hazus-MH MR5: Technical manual. Washington, DC: FEMA.
- FPHLM (Florida Public Hurricane Loss Model). 2015. "Florida public hurricane loss model." Accessed June 5, 2021. https://fphlm.cs.fiu.edu/index.html.
- Grayson, J. M., W. Pang, and S. Schiff. 2013. "Building envelope failure assessment framework for residential communities subjected to hurricanes." *Eng. Struct.* 51 (Jun): 245–258. https://doi.org/10.1016/j .engstruct.2013.01.027.
- Guo, Y., and J. van de Lindt. 2019. "Simulation of hurricane wind fields for community resilience applications: A data-driven approach using integrated asymmetric Holland models for inner and outer core regions." J. Struct. Eng. 145 (9): 4019089. https://doi.org/10.1061/(ASCE)ST .1943-541X.0002366.
- Hatzikyriakou, A., N. Lin, J. Gong, S. Xian, X. Hu, and A. Kennedy. 2016. "Component-based vulnerability analysis for residential structures subjected to storm surge impact from Hurricane Sandy." Nat. Hazards Rev. 17 (1): 5015005. https://doi.org/10.1061/(ASCE)NH.1527-6996 .0000205.
- He, J., F. Pan, and C. S. Cai. 2017. "A review of wood-frame low-rise building performance study under hurricane winds." *Eng. Struct.* 141 (Jun): 512–529. https://doi.org/10.1016/j.engstruct.2017.03.036.
- Henderson, D. J., and J. D. Ginger. 2007. "Vulnerability model of an Australian high-set house subjected to cyclonic wind loading." Wind Struct. 10 (3): 269–285. https://doi.org/10.12989/was.2007.10.3.269.
- Kakareko, G., S. Jung, S. Mishra, and O. A. Vanli. 2021. "Bayesian capacity model for hurricane vulnerability estimation." *Struct. Infra*struct. Eng. 17 (5): 638–648. https://doi.org/10.1080/15732479.2020 .1760318.
- Khajwal, A. B., and A. Noshadravan. 2020. "Probabilistic hurricane wind-induced loss model for risk assessment on a regional scale." ASCE-ASME J. Risk Uncertainty Eng. Syst. Part A: Civ. Eng. 6 (2): 4020020. https://doi.org/10.1061/AJRUA6.0001062.
- Li, Y., and B. R. Ellingwood. 2006. "Hurricane damage to residential construction in the US: Importance of uncertainty modeling in risk assessment." Eng. Struct. 28 (7): 1009–1018. https://doi.org/10.1016/j.engstruct.2005.11.005.
- Li, Y., J. W. van de Lindt, T. Dao, S. Bjarnadottir, and A. Ahuja. 2012. "Loss analysis for combined wind and surge in hurricanes." *Nat. Hazards Rev.* 13 (1): 1–10. https://doi.org/10.1061/(ASCE)NH.1527-6996.0000058.
- Lin, P., and N. Wang. 2016. "Building portfolio fragility functions to support scalable community resilience assessment." Sustainable Resilient Infrastruct. 1 (3–4): 108–122. https://doi.org/10.1080/23789689.2016.1254997.
- Masoomi, H., J. W. van de Lindt, M. R. Ameri, T. Q. Do, and B. M. Webb. 2019. "Combined wind-wave-surge hurricane-induced damage prediction for buildings." *J. Struct. Eng.* 145 (1): 4018227. https://doi.org/10 .1061/(ASCE)ST.1943-541X.0002241.
- Massarra, C. C., C. J. Friedland, B. D. Marx, and J. C. Dietrich. 2019. "Predictive multi-hazard hurricane data-based fragility model for residential homes." *Coastal Eng.* 151 (Sep): 10–21. https://doi.org/10.1016/j.coastaleng.2019.04.008.
- McCullough, M. C., A. Kareem, A. S. Donahue, and J. J. Westerink. 2013. "Structural damage under multiple hazards in coastal environments." J. Disaster Res. 8 (6): 1042–1051. https://doi.org/10.20965/jdr.2013.p1042.

- Memari, M., N. Attary, H. Masoomi, H. Mahmoud, J. W. van de Lindt, S. F. Pilkington, and M. R. Ameri. 2018. "Minimal building fragility portfolio for damage assessment of communities subjected to tornadoes."
 J. Struct. Eng. 144 (7): 4018072. https://doi.org/10.1061/(ASCE)ST.1943-541X.0002047.
- Mishra, S., O. A. Vanli, B. P. Alduse, and S. Jung. 2017. "Hurricane loss estimation in wood-frame buildings using Bayesian model updating: Assessing uncertainty in fragility and reliability analyses." *Eng. Struct*. 135 (Mar): 81–94. https://doi.org/10.1016/j.engstruct.2016.12.063.
- NOAA (National Oceanic and Atmospheric Administration). 2018. "Hurricane Florence 2018 forcast." Accessed November 12, 2020. https://www.nhc.noaa.gov/archive/2018/FLORENCE_graphics.php?product =5day cone no line.
- Nofal, O. M. 2021. High-resolution multi-hazard approach to quantify hurricane-induced risk for coastal and inland communities. Fort Collins, CO: Colorado State Univ.
- Nofal, O. M., and J. W. van de Lindt. 2020a. "High-resolution approach to quantify the impact of building-level flood mitigation and adaptation measures on flood losses at the community-level." *Int. J. Disaster Risk Reduct.* 51 (Dec): 101903. https://doi.org/10.1016/j.ijdrr.2020.101903.
- Nofal, O. M., and J. W. van de Lindt. 2020b. "Minimal building flood fragility and loss function portfolio for resilience analysis at the community level." Water 12 (8): 2277. https://doi.org/10.3390/w12082277.
- Nofal, O. M., and J. W. van de Lindt. 2020c. "Probabilistic flood loss assessment at the community scale: Case study of 2016 flooding in Lumberton, North Carolina." ASCE-ASME J. Risk Uncertainty Eng. Syst. Part A: Civ. Eng. 6 (2): 5020001. https://doi.org/10.1061 /AJRUA6.0001060.
- Nofal, O. M., and J. W. van de Lindt. 2020d. "Understanding flood risk in the context of community resilience modeling for the built environment: Research needs and trends." Sustainable Resilient Infrastruct. 5 (1): 1–17. https://doi.org/10.1080/23789689.2020.1722546.
- Nofal, O. M., and J. W. van de Lindt. 2021a. "Fragility-based flood risk modeling to quantify the effect of policy change on losses at the community level." Civ. Eng. Res. J. 11 (5): 555822. https://doi.org/10.19080 /CERJ.2021.11.555822.
- Nofal, O. M., and J. W. van de Lindt. 2021b. "High-resolution flood risk approach to quantify the impact of policy change on flood losses at community-level." *Int. J. Disaster Risk Reduct.* 62 (Aug): 102429. https://doi.org/10.1016/j.ijdrr.2021.102429.
- Nofal, O. M., J. W. van de Lindt, and T. Q. Do. 2020. "Multi-variate and single-variable flood fragility and loss approaches for wood frame buildings." *Reliab. Eng. Syst. Saf.* 202 (Oct): 106971. https://doi.org/10 .1016/j.ress.2020.106971.
- Nofal, O. M., J. W. van de Lindt, G. Yan, S. Hamideh, and J. C. Dietrich. 2021. "Multi-hazard hurricane vulnerability model to enable resilenceinformed decision." In *Proc., Int. Structural Engineering and Construc*tion (ISEC-11), edited by S. El Baradei, A. Madian, A. Singh, and S. Yazdani. Fargo, ND: ISEC Press. https://doi.org/10.14455/ISEC.2021.8 (1).RAD-01.
- Paleo-Torres, A., K. Gurley, J.-P. Pinelli, M. Baradaranshoraka, M. Zhao, A. Suppasri, and X. Peng. 2020. "Vulnerability of Florida residential structures to hurricane induced coastal flood." *Eng. Struct.* 220 (Oct): 111004. https://doi.org/10.1016/j.engstruct.2020.111004.
- Park, S., J. W. van de Lindt, and Y. Li. 2013. "Application of the hybrid ABV procedure for assessing community risk to hurricanes spatially." *Nat. Hazard.* 68 (2): 981–1000. https://doi.org/10.1007/s11069-013 -0674-2.
- Park, S., J. W. van de Lindt, and Li Yue. 2014. "ABV procedure combined with mechanistic response modeling for roof- and surge-loss estimation in hurricanes." *Perform. Constr. Facil.* 28 (2): 206–215. https://doi.org/10.1061/(ASCE)CF.1943-5509.0000397.
- Pei, B., W. Pang, F. Testik, and N. Ravichandran. 2013. "Joint distributions of hurricane wind and storm surge for the city of Charleston in South Carolina." In *Proc.*, ATC & SEI Conf. on Advances in Hurricane Engineering 2012, 703–714. Reston, VA: ASCE. https://doi.org/10 .1061/9780784412626.062.
- Pei, B., W. Pang, F. Y. Testik, N. Ravichandran, and F. Liu. 2014. "Mapping joint hurricane wind and surge hazards for Charleston, South Carolina."

- *Nat. Hazard.* 74 (2): 375–403. https://doi.org/10.1007/s11069-014-1185-5.
- Pinelli, J.-P., E. Simiu, K. Gurley, C. Subramanian, L. Zhang, A. Cope, J. J. Filliben, and S. Hamid. 2004. "Hurricane damage prediction model for residential structures." *J. Struct. Eng.* 130 (11): 1685–1691. https://doi.org/10.1061/(ASCE)0733-9445(2004)130:11(1685).
- Pita, G., J.-P. Pinelli, S. Cocke, K. Gurley, J. Mitrani-Reiser, J. Weekes, and S. Hamid. 2012. "Assessment of hurricane-induced internal damage to low-rise buildings in the Florida Public Hurricane Loss Model." J. Wind Eng. Ind. Aerodyn. 104 (Jul): 76–87. https://doi.org/10.1016/j.jweia .2012.03.023.
- Pita, G., J.-P. Pinelli, K. Gurley, and J. Mitrani-Reiser. 2015. "State of the art of hurricane vulnerability estimation methods: A review." *Nat. Haz-ards Rev.* 16 (2): 4014022. https://doi.org/10.1061/(ASCE)NH.1527 -6996.0000153.
- Powell, M. D., et al.2010. "Reconstruction of Hurricane Katrina's wind fields for storm surge and wave hindcasting." *Ocean Eng.* 37 (1): 26–36. https://doi.org/10.1016/j.oceaneng.2009.08.014.
- Rosowsky, D. V., and B. R. Ellingwood. 2002. "Performance-based engineering of wood frame housing: Fragility analysis methodology." J. Struct. Eng. 128 (1): 32–38. https://doi.org/10.1061/(ASCE)0733-9445(2002)128:1(32).
- State of North Carolina. 2019. "North Carolina spatial data." Accessed November 12, 2020. https://sdd.nc.gov/.
- State of North Carolina, Office of the Governor. 2018. "Hurricane Florence recovery recommendations: Building communities stronger and smarter." Accessed November 12, 2020. https://files.nc.gov/ncosbm/documents/files/Florence_Report_Full.pdf.
- Stewart, S. R., and R. Berg. 2019. "National Hurricane Center tropical cyclone report: Hurricane Florence." Accessed November 12, 2020. https://www.nhc.noaa.gov/data/tcr/AL062018_Florence.pdf.
- Taggart, M., and J. W. van de Lindt. 2009. "Performance-based design of residential wood-frame buildings for flood based on manageable loss." J. Perform. Constr. Facil. 23 (2): 56–64. https://doi.org/10.1061 /(ASCE)0887-3828(2009)23:2(56).
- Tanaka, S., S. Bunya, J. J. Westerink, C. Dawson, and R. A. Luettich, Jr.. 2011. "Scalability of an unstructured grid continuous Galerkin based hurricane storm surge model." *J. Sci. Comput.* 46 (3): 329–358. https://doi.org/10.1007/s10915-010-9402-1.
- Tomiczek, T., A. Kennedy, and S. Rogers. 2014. "Collapse limit state fragilities of wood-framed residences from storm surge and waves during Hurricane Ike." *J. Waterw. Port Coastal Ocean Eng.* 140 (1): 43–55. https://doi.org/10.1061/(ASCE)WW.1943-5460.0000212.
- Tomiczek, T., A. Kennedy, Y. Zhang, M. Owensby, M. E. Hope, N. Lin, and A. Flory. 2017. "Hurricane damage classification methodology and fragility functions derived from Hurricane Sandy's effects in Coastal

- New Jersey." *J. Waterw. Port Coastal Ocean Eng.* 143 (5): 4017027. https://doi.org/10.1061/(ASCE)WW.1943-5460.0000409.
- Unnikrishnan, V. U., and M. Barbato. 2017. "Multihazard interaction effects on the performance of low-rise wood-frame housing in hurricane-prone regions." J. Struct. Eng. 143 (8): 4017076. https://doi. org/10.1061/(ASCE)ST.1943-541X.0001797.
- US Census Bureau. 2019. "QuickFacts: North Carolina." Accessed November 12, 2020. https://www.census.gov/quickfacts/NC.
- van de Lindt, J. W., and M. Taggart. 2009. "Fragility analysis methodology for performance-based analysis of wood-frame buildings for flood." *Nat. Hazards Rev.* 10 (3): 113–123. https://doi.org/10.1061/(ASCE) 1527-6988(2009)10:3(113).
- van Verseveld, H. C. W., A. R. van Dongeren, N. G. Plant, W. S. Jäger, and C. den Heijer. 2015. "Modelling multi-hazard hurricane damages on an urbanized coast with a Bayesian Network approach." *Coastal Eng.* 103 (Sep): 1–14. https://doi.org/10.1016/j.coastaleng.2015.05.006.
- Vickery, P. J., J. Lin, P. F. Skerlj, L. A. Twisdale, Jr., and K. Huang. 2006a. "HAZUS-MH hurricane model methodology. I: Hurricane hazard, terrain, and wind load modeling." *Nat. Hazards Rev.* 7 (2): 82–93. https://doi.org/10.1061/(ASCE)1527-6988(2006)7:2(82).
- Vickery, P. J., F. J. Masters, M. D. Powell, and D. Wadhera. 2009. "Hurricane hazard modeling: The past, present, and future." *J. Wind Eng. Ind. Aerodyn.* 97 (7–8): 392–405. https://doi.org/10.1016/j.jweia.2009.05.005.
- Vickery, P. J., P. F. Skerlj, J. Lin, L. A. Twisdale, Jr., M. A. Young, and F. M. Lavelle. 2006b. "HAZUS-MH hurricane model methodology. II: Damage and loss estimation." *Nat. Hazards Rev.* 7 (2): 94–103. https://doi.org/10.1061/(ASCE)1527-6988(2006)7:2(94).
- Wang, C., H. Zhang, K. Feng, and Q. Li. 2017. "Assessing hurricane damage costs in the presence of vulnerability model uncertainty." *Nat. Hazard.* 85 (3): 1621–1635. https://doi.org/10.1007/s11069-016 -2651-z.
- Wang, W. L., and J. W. van de Lindt. 2021. "Quantitative modeling of residential building disaster recovery and effects of pre- and post-event policies." Int. J. Disaster Risk Reduct. 59 (Jun): 102259. https://doi.org/10.1016/j.ijdrr.2021.102259.
- Wang, W. T. L., J. W. van de Lindt, H. Cutler, N. Rosenheim, M. Koliou, J. S. Lee, and D. Calderon. 2021. "Community resilience assessment of an EF-5 tornado using the IN-CORE modeling environment." In *Life-cycle civil engineering: Innovation, theory and practice*, edited by A. Chen, X. Ruan, and D. M. Frangopol, 394–398. Boca Raton, FL: CRC Press.
- Zhang, W., P. Lin, N. Wang, C. Nicholson, and X. Xue. 2018. "Probabilistic prediction of postdisaster functionality loss of community building portfolios considering utility disruptions." J. Struct. Eng. 144 (4): 4018015. https://doi.org/10.1061/(ASCE)ST.1943-541X.0001984.